



GIS-Based Culvert Design

ENFO410
LUKE WILSON

Acknowledgements

I would like to thank Professor Rien Visser and PhD candidate Campbell Harvey for their guidance, insight and help for the duration of this study. I would also like to acknowledge both Riki Green and Paul Thompson from Summit Forests NZ Ltd; Riki Green for the idea and discussion that ignited my interest in the study and Paul Thompson for providing the LiDAR data required to undertake this study.

Abstract

While sizing culverts for a given flood flow is relatively straightforward, predicting the design flood flow can be complex. Several assumptions are required in the prediction and some NES-PF approved methods were developed prior to computers to undertake it. The purpose of the study was to determine the feasibility and practicality of GIS-based culvert design. The key aims were to streamline existing flood flow calculations to provide consistent and accurate results independent of the user.

A workflow was developed using ModelBuilder in ArcGIS and python (ArcPy) to semi-automate the calculation of design flood flow using the Rational and TM61 methods. Equations were sourced from literature, but parts of the process required the use of polynomial approximation to replace nomograms (chart derived values). The workflow utilized three key sources of spatial data including LiDAR elevation, and the LCDB and FSL soil drainage layers. The latter two sources of spatial data allowed the runoff coefficient C and cover coefficient W_{ic} to be calculated. The workflow developed for these two coefficients also means that a user can estimate the effect of either clear-cut, or partial harvest of the forest in the catchment, on the predicted flood flow. It was felt that the new methodology developed for calculating these coefficients allowed for a better design by being more structured and reducing the reliance on user 'experience' in determining an appropriate value.

In total, the process was tested on 35 catchments across the Northland region of New Zealand, with an average catchment size of 161 ha. Both the equations and polynomials performed very well for the ranges they were evaluated, typically being less than 2% different to the same value derived manually. When using the same interpretations, the flood flow was only 3.5% different between the manual and semi-automated process. The semi-automated process removed a large amount of potential human error while also saving time.

The equations in the GIS model can be modified to suit the interpretation of the factors. For example, for 'average stream slope', there are several possible interpretations. This is used directly in the flood flow equation and indirectly in that it is part of the time-of-concentration equation. The RamserKirpich time-of-concentration equation presented in the TM61 method, commonly used in New Zealand, refers to 'average channel slope' – for which the equal area method is suggested. Kirpich (1940) provides two methods (in US imperial units) for determining slope; one using a height difference-flow length ratio and the other, average catchment height (above outlet) to catchment area ratio. A common interpretation for our forest industry applications is the average slope of the longest 'blue-line' stream channel in the catchment as shown on the LINZ Topographic 1:50,000 series maps.

When comparing the GIS model using the average stream slope with the TM61 equal area slope method, it was 0.034m/m greater (or 41% steeper). This then caused a significant difference in the flood flow estimate (approx. 30% different), showing how sensitive the overall equation is to the interpretation of 'average stream slope'. While further work is needed to determine the most appropriate measure of channel slope, this study highlighted that the process of GIS-based culvert design is both physically feasible and practical, underlining further potential to expand on and employ the work completed in this study.

Table of Contents

Acknowledgements.....	i
Abstract.....	ii
1. Introduction	1
2. Literature Review.....	1
2.1 National Environmental Standards for Plantation Forestry	1
2.2 Engineering Design Manual	2
Section 8.5: Single Culvert River Crossings	2
Section 8.9: Prediction of flood flows and sizing culverts	3
2.3 Culvert Design	4
2.4 Rational Method	8
2.4.1 C Factor	9
Rational Method in GIS	12
2.5 TM61	14
2.5.1 Time of Concentration	16
2.6 Regional.....	18
3. Objectives.....	18
4. Methodology.....	19
4.1 Software and Data Sources.....	19
4.2 Rational Method	20
Semi-Automated Process.....	20
Manual Process Rational.....	24
4.3 TM61	26
Semi-Automated	26
Manual Process TM61.....	29
Culvert Calculations	32
5. Results and Analysis.....	33
5.1 Catchment characteristics	33
5.1.1 Location.....	33
5.1.2 Catchment Area	33
5.1.3 Channel Slope	35
5.1.4 Channel Slope and Flow Rate.....	37
5.2 Time of Concentration	41

5.3 Equation evaluation	43
5.4 Time Evaluation.....	45
5.5 Runoff Coefficient	48
6. Discussion.....	51
6.1 Channel Slope	51
6.2 Time of Concentration	53
6.3 Equations	54
6.4 Time Evaluation.....	55
6.5 Runoff Coefficient	55
7. Conclusion.....	56
References	58
Appendices.....	a
Appendix A: Python Code	a
Appendix B: Runoff Coefficient Processes	b
Part 1:.....	b
Part 2:.....	b

1. Introduction

Stream and river crossing design is a critical part of forest road construction. These waterway crossings must be designed correctly to meet expected environmental requirements due to the potential adverse effects on the waterways a crossing can have (Brown & Visser, 2017). Alongside the environmental considerations, it is vital that these crossings also meet the operation's needs and make economic sense. Where a crossing is needed, it needs to be designed stringently (NZFOA, 2020).

NZFOAs (2020) New Zealand Forest Road Engineering Manual gives the different structures that are appropriate to allow access across a waterway. These structures include fords, temporary crossings, single culverts, battery culverts, drift decks and single-span bridges. This study will focus on the calculation of design flood flows which are required to assess what type of structure is required. Flow is defined here as the volume of water passing a specified point at a given instance in time and is measured in cumecs (m^3/s). There are three standard methods used in New Zealand to calculate the streamflow. These include the rational, technical memorandum No. 61 (TM61) and regional methods (NZFOA, 2020). The flood flows calculated during the study will be applied solely to the design of single culverts. It is noted, however, that the flood flows produced could also be applied to the design of the other structures if it were required.

Currently, the forest industry use a mixture of methods to undertake the waterway crossing design process. These methods can include GIS to determine catchment parameters, spreadsheets to perform calculations and charts to obtain the required design parameters. These mixtures of methods are evident in both the dissertation projects of Costley (2018) and McCormack (2020). An initial purpose for this study was developed from the thought that this current process is somewhat disjointed, and a more uniform process could be designed to streamline existing workflows and save time. Other initial focus points identified include the design of smaller catchments, single culverts (as stated above) and performing the analysis in the region of Northland.

2. Literature Review

2.1 National Environmental Standards for Plantation Forestry

The New Zealand Government first discussed the National Environmental Standards for Plantation Forestry (NES-PF) in 2010 as regulations under the Resource Management Act (RMA). Work continued to develop the standards between 2010 and 2017, with several drafts and versions being completed (Ministry for the Environment, 2018). On the third of August 2017, the NES-PF was published, however, it wasn't till the first of May 2018 until it came into effect (Ministry for Primary Industries, 2020).

The purpose and reasoning behind the development of the NES-PF was detailed by the forestry minister of the time, Hon Shane Jones. "Forestry is our third largest primary industry, but its efficiency has been hindered by variation in planning rules across New Zealand's multitude of councils. Many large forests cover multiple council boundaries, resulting in different rules for the same forest. From today that forest will be governed by one set of rules" (Jones, 2018).

Before the NES-PF came into effect, a forested area was governed by the regional councils and territorial authorities in which it lay. Both of these organizations have plans associated with how activities are to be undertaken. These plans detail the rules related to the activities and whether compliance needed to be sought. The plans are considerable documents numbering in the hundreds of pages. Therefore, the difficulty with navigating these plans, especially if the forested area is spread over several different

regional councils or territorial authorities, becomes very difficult (Pendly et al., 2015). The NES-PF prevails over district or regional plans except where it allows the plans to employ more stringent rules (Ministry for Primary Industries, 2020).

The NES-PF covers eight core plantation activities, including river crossings (Ministry for Primary Industries, 2020). The NES-PF implications on culvert design are given in regulation 45(1) and 46(1). Regulation 45(1) provides the preferred design procedures for performing the flood flow estimations. It is stated in the NES-PF that one or more of the following design procedures must be used for flood estimation:

- Flood Estimation – A Revised Design Procedure.
- Technical Memorandum Number 61.
- Comparison of a regional method for estimating design floods with two rainfall-based methods.

From regulation 46(1), the clauses that are of interest and have implications for this study are a and b. These clauses follow:

- (a) The calculated 5% AEP storm flow from the catchment above the river crossing point must be no greater than 5.5 m³ per second.
- (b) The culvert must be designed to pass a 5% AEP flood event without heading up.

2.2 Engineering Design Manual

The New Zealand Forest Road Engineering Manual was first published in 1999 by the Logging Industry Research Association. Subsequent revisions occurred from the New Zealand Forest Owners Association (NZFOA) in 2012 and most recently 2020 to include the changes brought forth by the introduction of the NES-PF. The manual provides a comprehensive guide for people with a limited engineering background and a source of reference material for forest roading supervisors and engineers (NZFOA, 2020).

The sections of interest in the manual related to this study are 8.5 and 8.9. Section 8.5 outlines information for single culvert river crossings and covers aspects like design, types, installation and how to minimise the chances of them failing. Section 8.9 outlines three methods for calculating flood flows and one method for calculating culvert size using a nomogram.

Section 8.5: Single Culvert River Crossings

Single culverts are easy to install, relatively cheap compared to other alternatives and are most commonly used to cross small to medium-sized rivers on forestry roads. Typically, there are two types of materials used for single pipe crossings, plastic and reinforced concrete. Both these materials have a typical style, with the plastic pipes being corrugated and the concrete pipes being smooth.

Plastic corrugated pipes are commonly used. However, they do have some disadvantages compared to the smooth reinforced concrete pipes. These disadvantages include a lower water discharge capacity, a reliance on the soil envelope to provide strength, often get damaged during installation, and are subjected to abrasions which make them less durable.

Comparatively, reinforced concrete pipes have excellent hydraulic characteristics and are great for applications where a significant load-bearing capacity is required. They are durable and last a long time without corroding or losing their structural strength, are less dependent on the soil envelope and can be

reused easily. However, there are some significant disadvantages associated with concrete pipes, which include difficulty establishing fish passage and a high supply and installation cost.

The culvert design requirements specified in this section include determining the flow rate and water depth associated with a 1-in-20-year storm event. The designed culvert should also be able to pass this event without heading up. Heading up helps to push water through a culvert and refers to the level at which the water is above the culvert's top. If designing to the permitted category of the NES-PF, a heading-up ratio of 1 should be selected. The heading-up ratio is the depth of the water divided by the culvert diameter. There are many different things to consider when designing a culvert, a list of which follows.

- Expected flood flows and probability of these occurring.
- The significance of the forestry road where the culvert will be installed. Spur road verse arterial.
- Catchment parameters including size, geology, topography and cover.
- The risk of adverse upstream and downstream effects.
- Designed where possible to include an overland path so if the culverts maximum capacity is exceeded, damage can be potentially avoided.
- Both the upstream and downstream fish passage.
- The potential and amount of woody debris reaching the culvert.
- The specific location of the culvert.
- Location on a straight section of a waterway to reduce scour (if possible).
- Where possible to avoid placing the culvert where the natural course and gradient of the waterway is altered.

Section 8.9: Prediction of flood flows and sizing culverts

To ensure an appropriately designed waterway crossing, both the design peak discharge and the capacity of the waterway crossing to pass the designed flood flow need to be established. Section 8.9 explains these two design parameters. Flood flows are commonly given as cumecs or cubic meters of water per second. The flood flows are also defined for an annual exceedance probability (AEP) or a specified return period. The relationship between AEP and return period follows in equation 1.

$$AEP (\%) = \frac{1}{Return\ Period} \times 100 \quad (1)$$

The prediction of flood flows is not an exact science, and as such, the design and selection of a value for a site must be completed carefully. There are three methods specified by the design guide to calculate design peak discharge in New Zealand. These three methods are the regional, technical memorandum No. 61 (TM61) and rational. Both the rational and TM61 methods are classed as empirical methods. Empirical methods use rainfall intensity of a given duration alongside catchment and river channel characteristics to predict flood flows. Comparatively to these empirical methods, a regional method draws from data gathered over time from river gauging stages. The data is then fitted to observed flood flows and extrapolated to catchments with no raw data collection (NZFOA, 2020).

The derivation of a flood flow estimate for an appropriate annual exceedance probability allows a suitable culvert size to be determined. The flow rate of water is dependent on several factors, including its diameter, length, slope, the material it is made from, and the pressure the water is under if it is allowed to head up. The pressure the water is under should be a design parameter of limited use as under the

permitted category of the NES-PF culverts are not allowed to head up. The sizing of the culvert diameter is achieved using a simplified chart (nomogram). The nomogram relates the culvert type, heading up ratio and three different scales to allow the culvert sizing based on the flood flows to be determined (NZFOA, 2020).

Section 8.9 of The New Zealand Forest Road Engineering Manual also gives another method of determining culvert sizing using a risk-based approach. A comparison is made between the culvert's required design life, and the appropriate risk of the forest managed. These two parameters are then used to give the reoccurrence level flood event used in the design.

2.3 Culvert Design

The typical design of culverts is done using nomograms (charts). A nomogram consists of several lines of a given scale and allows a graphical computation of a function. A nomogram is arranged so that a straight line can connect known values on two lines to an unknown value on another line, allowing the unknown value to be determined (NOMOGRAM, n.d.). Costley (2018) found through an industry survey that eight out of ten surveyed forestry employees used charts (nomograms) to determine an appropriately sized culvert, with the remaining two using spreadsheets. Allum et al. (2020) stated that the use of charts to calculate culvert sizing is commonly taught at the University of Canterbury forestry school and is widely used in industry.

The nomogram presented in The New Zealand Forest Road Engineering Manual is sourced from pages 84-86 of Keller and Sherars (2003) Low Volume Roads Engineering Best Management Practices and Field Guides. Typical factors which influence culvert flow includes the inlet and outlet flow, and more specifically, the culverts entrance, slope and headwater (Allum et al., 2020). The nomograms presented in The New Zealand Forest Road Engineering Manual are based on inlet control.

Inlet control occurs when the culvert barrel has excess capacity to carry more flow (water), but instead, the flow is governed by the culvert's entrance. Simply, the water can flow quicker through the culvert than it can enter it (Allum et al., 2020). The flow occurring in a culvert under inlet control is a shallow and high-velocity flow that is classed as supercritical. Due to inlet control only being impacted on the upstream end of a culvert, only two parameters significantly affect it. The two parameters that will impact the culverts' performance are the headwater depth and the inlet style. The headwater depth is the depth of water above the culvert inlet bottom. The inlet style is affected by its area and edge configuration. The inlet area relates to the culvert's cross-sectional area, and the edge configuration describes its entrance type. There are several different entrance types, a few of which include mitered, protruding, and headwalls and wingwalls (Normann et al., 1985).

Outlet control, on the other hand, occurs when the inlet opening accepts more flow than the culvert barrel can convey. Subsequently, the culvert barrel does not have any excess capacity and governs the flow through the culvert. The flow occurring in a culvert under outlet control is classed as subcritical and is relatively deep, and has a lower velocity. The factors which influence inlet control also have an impact on outlet control. In addition to these factors, the barrel characteristics (roughness, area, shape, length and slope) and tailwater elevation also impact the culverts performance under outlet control. The barrel's roughness relates to the material it is made out of and is represented by a hydraulic resistance coefficient. The downstream water surface elevation determines the tailwater elevation characteristic of the culvert. A summary of influencing factors for inlet and outlet flows follows in table 1.

Table 1. The inlet and outlet flow summary of influencing factors (Normann et al., 1985).

Factor	Inlet Control	Outlet Control
Headwater Elevation	✓	✓
Inlet Area	✓	✓
Inlet Edge Configuration	✓	✓
Inlet Shape	✓	✓
Barrel Roughness	×	✓
Barrel Area	×	✓
Barrel Shape	×	✓
Barrel Length	×	✓
Barrel Slope	*	✓
Tailwater Elevation	×	✓
* Barrel slope affects inlet control performance to a small degree, but may be neglected.		

Table 1 provides an easy comparison between the influencing factors of each of the control methods. The charts presented for culvert design, based on inlet control, in the NZFOA (2020) New Zealand Forest Road Engineering Manual, follow in figures 1 and 2.

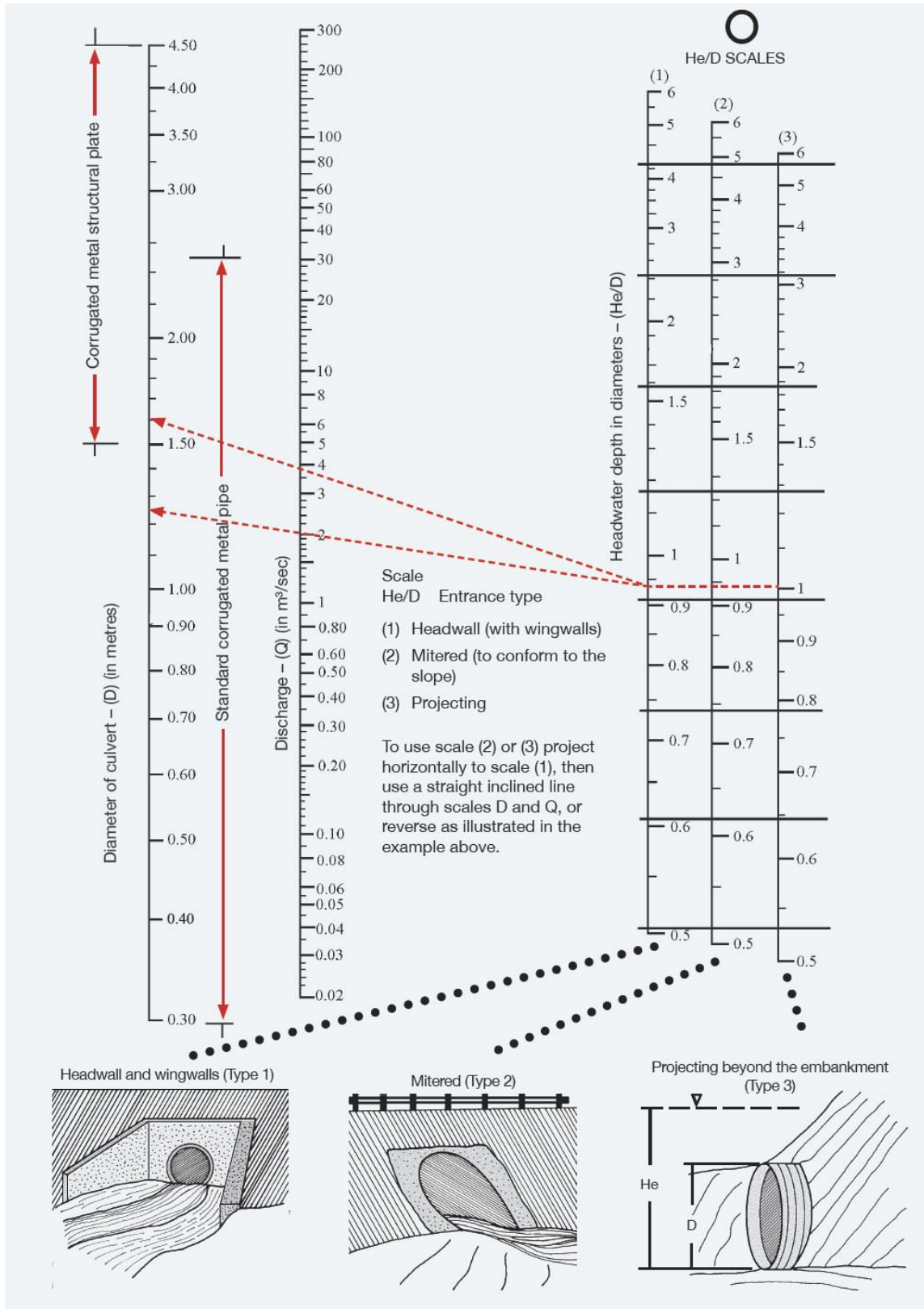


Fig 1. Nomogram for culvert sizing for a corrugated metal pipe with inlet control (Keller & Sherar, 2003).

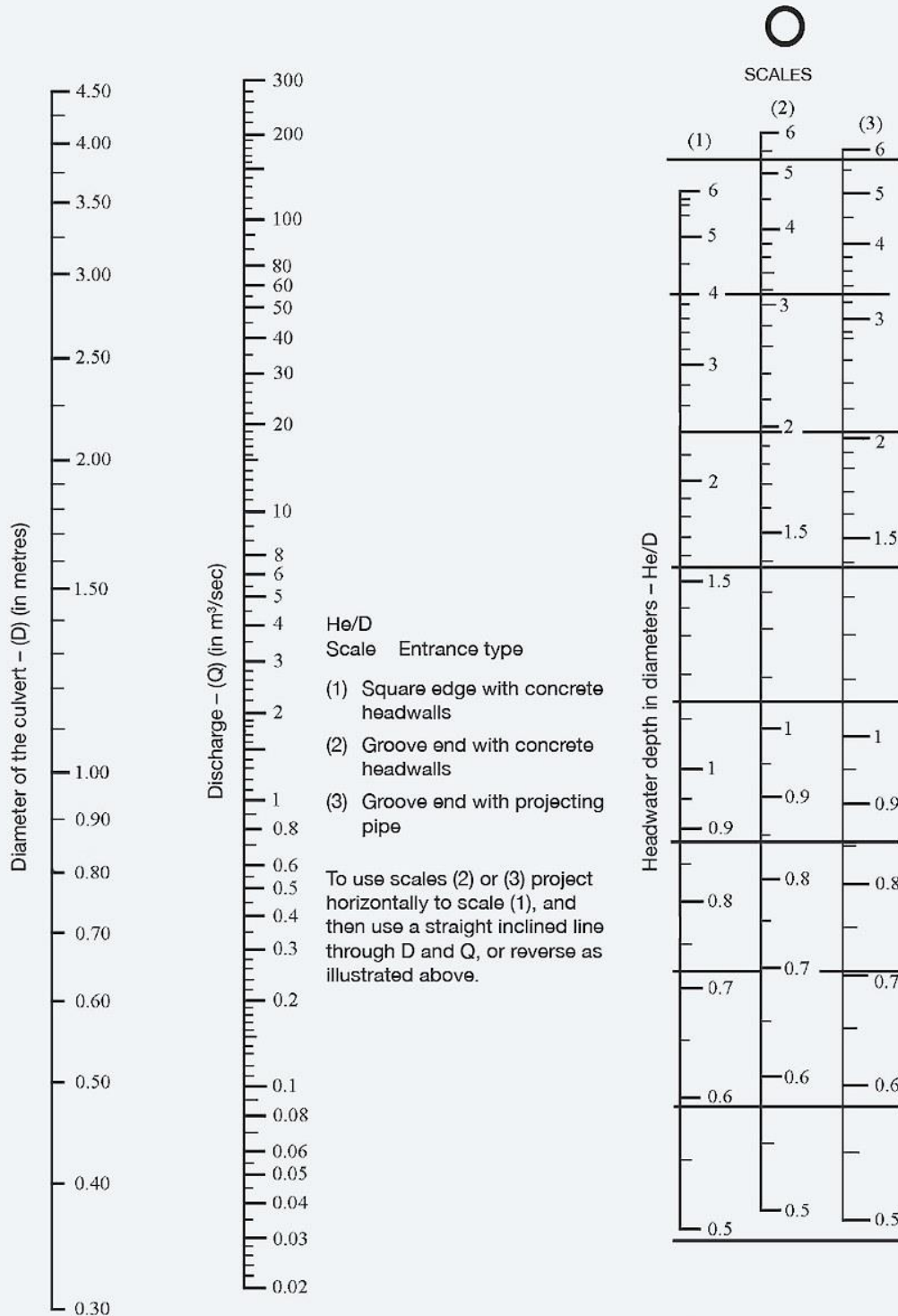


Fig 2. Nomogram for culvert sizing for a concrete pipe with inlet control (Keller & Sherar, 2003)

2.4 Rational Method

The rational method for determining peak discharge was developed in Ireland by Thomas Mulvany in 1851 (Dooge, 1974), and by 1889 its use was rampant in North America (Hydrology Studio, n.d.). The method's name was derived from the fact that its units have been 'rationalised' (Smart, 2004). The rational method is classed as an empirical equation (NZFOA, 2020). An empirical equation is formed from observations and experiences rather than theoretical means (The Engineering Toolbox, 2008). The equation of the rational method as given in NZFOAs (2020) New Zealand Forest Road Engineering Manual follows as equation 2:

$$Q = \frac{CiA}{362} \quad (2)$$

Where,

Q = peak discharge (m³/s)

C = rational runoff coefficient (dimensionless)

i = rainfall intensity (mm/hr) – for a calculated time of concentration (in minutes)

A = catchment area (ha)

The rational method's main draw is its simplicity (NZFOA, 2020; Hydrology Studio, n.d.). However, there are several assumptions that this method makes and subsequently, it also has some limitations. Notable key limitations and assumptions of the rational method include:

- Rainfall intensity is uniform throughout the duration of the storm across the entire catchment (NZFOA, 2020; Thomason, 2019).
- The catchment is impervious - does not account for storage (NZFOA, 2020; Thomason, 2019).
- The whole catchment contributes to runoff (NZFOA, 2020).

Both NZFOA (2020) and Thomason (2019) further state that the above assumptions are reasonable for small catchments. The maximum size catchment the rational method can be applied to according to NZFOA (2020), and Thomason (2019) is 120ha and 200ac (approximately 80ha), respectively. The difference in the maximum catchment size applicable to the rational method is common in literature. It is thought that a potential difference here was that Thomason (2019) was designing for catchments in North America, whereas NZFOA (2020) were designing for catchments in New Zealand. To gauge an appropriate maximum catchment size for the rational method, a comparison between the size limits and the location they were applied to, from different literature sources, follows in table 2.

Table 2. The rational methods maximum catchment size limitation.

Size of Catchment Appropriate (ha)	Study Location	Source
120	New Zealand	(NZFOA, 2020)
80	North America	(Thomason, 2019)
50	New Zealand	(Environmental Hazards Group, 2012)
80	South Africa	(HRU, 1972)
2500	New Zealand	(Ministry of Works and Development, 1978)
120	North America	(Keller & Sherar, 2003)

The variations in an appropriate upper limit for catchment size tended to be of a similar magnitude excluding the Ministry of Works and Development (1978). The New Zealand Forest Road Engineering

Manual from 2011 also stated that the upper limit for catchment size was 2500ha (Costley, 2018). This version has been updated and now gives the upper limit shown in table 2 of 120ha (NZFOA, 2020). The change in this upper limit highlights renewed thinking around the appropriate catchment size limit for this method. Given the variability in maximum catchment size relating to the rational method, as shown in table 2, a definitive choice based on the literature consulted cannot be specified. However, to best align the design process to that of the New Zealand forest industry, a maximum catchment extent of 120ha, as specified by NZFOA (2020), will be used in this study.

The High Intensity Rainfall Design System V4 from NIWA (n.d.) is used to provide the data required for determining the rainfall intensity across a catchment. The rainfall intensity selected is for a specified duration and frequency and represents the average rainfall rate in mm/hr. The duration of the rainfall event is assumed to equal the time of concentration, in minutes, of the catchment in question (Thomason, 2019). The implication of selecting the correct method to determine the time of concentration is crucial due to the significant impact it has on the design storm chosen. This implication is further reinforced by Smart (2004), who states that while the rational method appears simple, the 'correct' selection of both the intensity (i) and the runoff coefficient (C) is hugely important in determining the overall effectiveness of the method.

The importance of selecting a correct 'C' value was also highlighted by Pennington (2012) and Christchurch City Council (2020). Both Pennington (2012) and the Christchurch City Council (2020) emphasised that the rational method must be used with caution due to how sensitive it is to the selection of the runoff coefficient.

2.4.1 C Factor

The runoff coefficient (C) represents a simple ratio between the rainfall which occurs across the catchment and the runoff this creates (NZFOA, 2020; Oregon.gov, 2014). The runoff coefficient varies due to the interactions of many complex catchment properties, including storage, infiltration, antecedent moisture, ground cover, slope and soil types (Christchurch City Council, 2020; Oregon.gov, 2014). The C value differs depending on the surface type and ranges between 0 - 1 (Oregon.gov, 2014; Thomason, 2019). The implication that the runoff coefficient has can be easily discerned from the range it occurs over. The closer to one the value of the coefficient is, the more runoff that occurs across the catchment. Conversely, the closer to zero the coefficient is, the less runoff that occurs across the catchment. The implication of selecting a correct C factor can thus be easily distinguished due to its huge impact on the peak discharge estimated.

Given the importance of selecting the runoff coefficient, it is thought that there would be a straightforward design methodology given for selecting one in the NZFOA (2020) New Zealand Forest Road Engineering Manual. However, currently, there is none provided. Guidance is provided by the manual around the selection of a coefficient when clear-felling a catchment. The Manual highlights that if an entire catchment is to be clear-felled over a two to three-year period, then it is prudent to choose higher C values. The manual further extrapolates this point and states that if the entirety of a small catchment is clear-felled, it is appropriate to use a C value equal to one (NZFOA, 2020).

The NZFOA (2020) New Zealand Forest Road Engineering Manual also referenced Chapter 5 of Keller and Sherar (2003) *Hydrology for Drainage Crossing Design* as a further reference for runoff coefficient information. Upon investigating Keller and Sherar (2003), the method of selecting an appropriate runoff

coefficient was stated as “The designer must develop experience and use judgment to select the appropriate value of C within the range shown”. This statement further highlights a lack of a specific design procedure for selecting a runoff coefficient and highlights how there can be significant discrepancies when the rational method is used due to differing techniques and experience levels. The lack of a specified design procedure around the runoff coefficient selection indicates a potential knowledge gap and room for further research to be conducted in this area.

The potential knowledge gap was further evaluated by searching for other New Zealand-based literature around selecting an appropriate runoff coefficient. The Waterways, Wetlands and Drainage Guide from the Christchurch City Council (2020) simply stated that the runoff coefficient should be based on the likely conditions that will exist after the catchment has been developed. Which, once again, highlights a lack of a clear and succinct design process.

Two North American design guides (Oregon and Texas) reinforced the lack of design procedure for the runoff coefficient selection with both guides presenting a clear and structured methodology for undertaking it (Oregon.gov, 2014; Thomason, 2019). The guidelines highlighted a similar technique to deal with a catchment of mixed land use, which involved developing a weighted runoff coefficient. The weighted runoff coefficient is calculated by summing the product of the land-use area and the respected coefficient and then dividing by the total area. Both guides had an identical equation differing only in format and variable definition. Of the two, Thomason’s (2019) equation was defined the best and follows as equation 3:

$$C_w = \frac{\sum_{j=1}^n C_j A_j}{\sum_{j=1}^n A_j} \quad (3)$$

Where;

C_w = the weighted runoff coefficient.

C_j = runoff coefficient for area j.

A_j = area for landcover j.

N = number of distinct land covers.

Thomason (2019) also highlighted another method for rural and mixed-use watersheds. The runoff coefficient is split into four aspects, each of which contributes to form the overall design value. The four watershed characteristics pertain to components accounting for watershed relief, soil infiltration, vegetal cover and surface type. The overall runoff coefficient is the summation of these four contributing factors. The four aspects are also subdivided into four categories which include extreme, high, normal and low. The technique highlighted above was also used in a New Zealand application by Griffiths and McKerchar (2012). Both sources provide relevant tables to allow the determination of the four aspects. The table of runoff coefficients as supplied by NZFOA (2020) New Zealand Forest Road Engineering manual follows in figure 3.

Rational method values of "C"	
Land use or type	"C" value
Agriculture	
Bare soil	0.20-0.60
Cultivated field (sandy soil)	0.20-0.40
Cultivated fields (clay soil)	0.30-0.50
Grass	
Turf, meadows	0.10-0.40
Steep grassed areas	0.50-0.70
Woodland/forest	
Wooded areas with level ground	0.05-0.25
Forested areas with steep slopes	0.15-0.40
Bare areas, steep and rocky	0.50-0.90

Fig 3. Runoff coefficient table as provided in the NZ Forest Road Engineering manual as sourced from Keller and Sherar (2003).

The table of coefficients given above in figure 3 is quite basic. As a result, employing the values given in classifying a runoff coefficient leaves a lot of interpretation open to the designer. However, there are more specific guides that aid in the selection of appropriate runoff coefficient values, one of which follows in figure 4.

Description of Surface	C
Natural surface types	
Bare impermeable clay with no interception channels or run-off control	0.70
Bare uncultivated soil of medium soakage	0.60
Heavy clay soil types:	
• pasture and grass cover	0.40
• bush and scrub cover	0.35
• cultivated	0.30
Medium soakage soil types:	
• pasture and grass cover	0.30
• bush and scrub cover	0.25
• cultivated	0.20
High soakage gravel, sandy and volcanic soil types:	
• pasture and grass cover	0.20
• bush and scrub cover	0.15
• cultivated	0.10
Parks, playgrounds and reserves:	
• mainly grassed	0.30
• predominantly bush	0.25
Gardens, lawns etc	0.25
Developed surface types	
Fully roofed and/or sealed developments	0.90
Steel and non -absorbent roof surfaces	0.90
Asphalt and concrete paved surfaces	0.85
Near flat and slightly absorbent roof surfaces	0.80
Stone, brick and precast concrete paving panels:	
• with sealed joints	0.80
• with open joints	0.60
Unsealed roads	0.50
Railway and unsealed yards and similar surfaces	0.35
Land use types	
Industrial, commercial, shopping areas and town house developments	0.65
Residential areas in which the impervious area is less than 36% of gross area	0.45
Residential areas in which the impervious area is 36% to 50% of gross area	0.55

Fig 4. More detailed and specific runoff coefficients (Environmental Hazards Group, 2012; Department of Building and Housing, 2020).

Figure 4 gives more comprehensive values for the runoff coefficient and includes soil type into the design process, increasing the detail required to perform the classification. Environmental Hazard Group (2012) have adapted the coefficients from the Department of Building and Housing (2020). The Department of Building and Housing (2020) also provides a set of corrections to the runoff coefficient to incorporate the effect of slope. The slope correction factors follow in figure 5.

The runoff coefficients are to be modified for slope as follows¹:

- -0.05 for Slope < 5%
- No adjustment for 5%<Slope<10%
- +0.05 for 10%<Slope<20%
- +0.10 for Slope>20%”

Fig 5. Runoff coefficient adjustments for slope.

The process of using more detailed runoff coefficients based on both soil and slope characteristics is commonly referred to in literature as the revised/adjusted rational method. The more specific coefficients and the fact the effects of slope and soil characteristics have been included means that it is likely they can be employed more effectively and accurately than those of the standard rational method shown in figure 3 (Costley, 2018).

Rational Method in GIS

The implementation of the rational method into ArcGIS has been undertaken both fully and partially in several studies overseas. However, there was no literature identified which completed the process in New Zealand highlighting an opportunity to fill a local knowledge gap. Blagojević et al. (2018) used GIS to develop a coefficient map for catchments in the Bosnia and Herzegovina regions. The process they undertook to achieve their results was well documented and could be replicated if needed. Figure 6 follows and shows the workflow Blagojević et al. (2018) undertook.

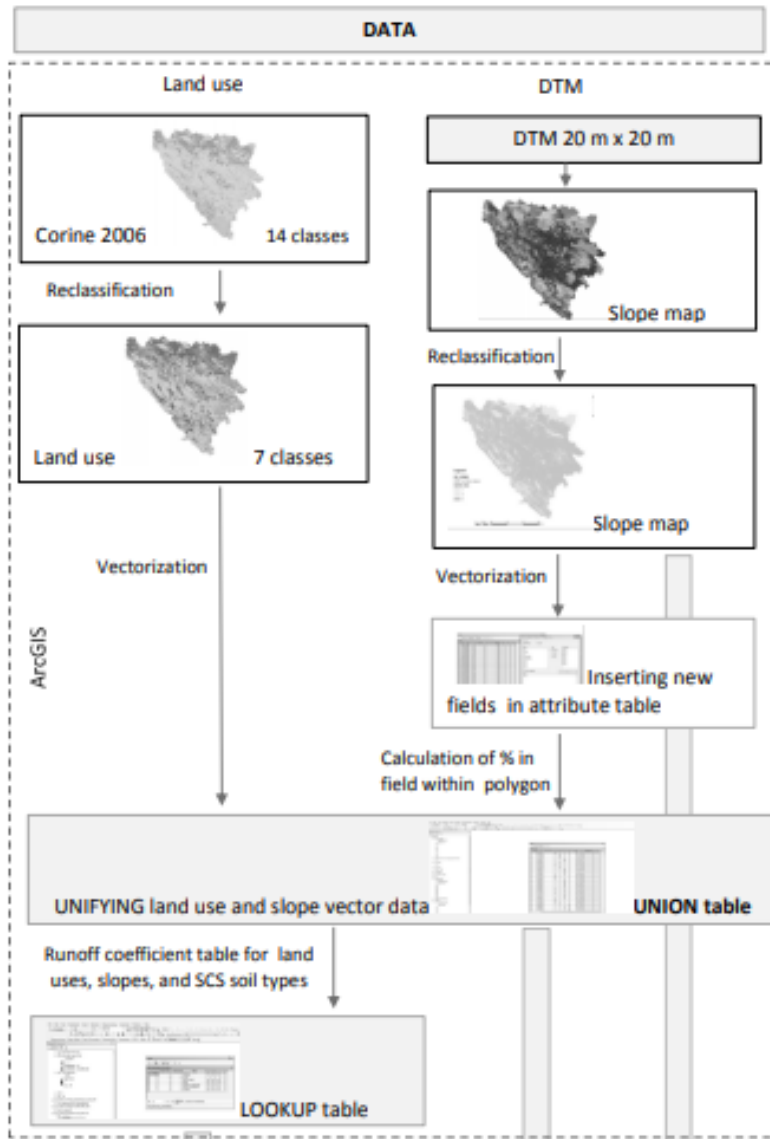


Fig 6. Blagojević et al. (2018) process undertaken to produce a coefficient map.

The lookup table specified as the output was then put into HEC-GeoHMS to produce a coefficient map. HEC-GeoHMS (Geospatial Hydrological Modelling Extension) is a geospatial hydrology tool kit add on to ArcGIS (US Army Corps of Engineers, n.d.). Blagojević et al. (2018) also developed their runoff coefficient using a composite classification similar to equation 3 above.

Greer et al. (2018) undertook a project in Tuscaloosa, Alabama, to perform GIS-enabled culvert design. The implementation of methods into GIS was achieved by creating a tool using the programming language python. Python scripts can be added into ArcGIS to provide additional functionality and to develop unique processing tools. The authors also used a Python site package ArcPy to perform geoprocessing and spatial operations within a python environment. Figure 7 follows and shows the workflow used by the authors.

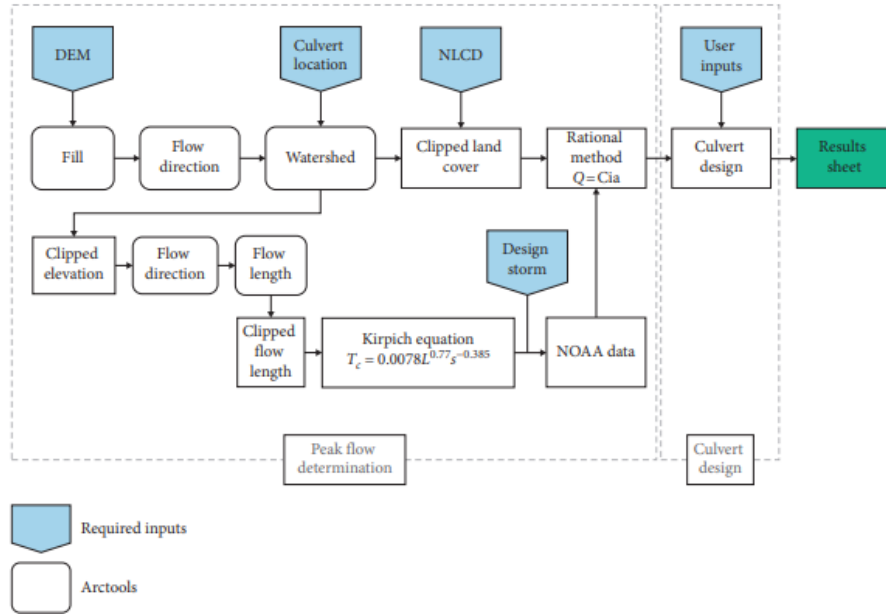


Fig 7. Workflow used to perform culvert calculations within the GIS environment (Greer et al., 2018).

Greer et al. (2018), like Blagojević et al. (2018), also used a composite method to determine the runoff coefficient across the catchment. The methodology used by Greer et al. (2018) provides a valuable basis from which to develop a similar methodology to implement the rational method into GIS.

2.5 TM61

Technical Memorandum 61 (TM61) is a variant of the rational method developed by the Ministry of Works in 1953 for use in smaller catchments. TM61 uses the catchment area, channel length, average channel slope, direct length (straight line distance from the culvert to the most distant point in the catchment), rainfall depth (equal duration to the catchment time of concentration), and general information about soil type, topography and land cover to estimate the flood flow of a catchment (NZFOA, 2020). The Ministry of Works and Development (1980) was the original publication for the TM61, and the equation it gave to determine an estimate of peak discharge follows as equation 4:

$$Q_p = 0.0139CRSA^{0.75} \quad (4)$$

Where,

- Q_p = the estimate of the design peak discharge (m³/s).
- C = a coefficient depending on the physiography of the catchment.
- R = rainfall factor depending on the design storm.
- S = catchment shape factor.
- A = catchment area (km²).

The runoff coefficient for the TM61 method uses the product of a slope factor and another factor which accounts for infiltration, ground surface and cover characteristics effects on runoff (Ministry of Works and Development, 1980). The difference between the vigour at which the runoff coefficient is chosen through the TM61 method and the standard rational method is readily apparent. The Ministry of Works and Development (1980) gives a special mention to the two factors importance in determining an appropriate runoff coefficient due to their impact on the design discharge estimate. The rainfall factor R is given by equation 5:

$$R = \frac{\text{design rainfall depth}}{\text{standard rainfall depth}} \quad (5)$$

The rainfall depth depends on both the return period and duration of the design storm. The design storm's duration is calculated using the same process as the rational method, the time of concentration. Once again, the time of concentration plays a vital role in determining an accurate design discharge. The standard rainfall depth is calculated using a standard curve.

The catchment shape factor (S) is calculated using a nomogram. A dimensionless number (k) is used to find the intersection point on the given curve, which allows the shape factor to be determined. The equation for K is given by equation 6:

$$K = \frac{A}{L_d^2} \quad (6)$$

Where,

A is the area of the catchment in square kilometres.

L_d is the direct length of the catchment in kilometres (straight line distance from the culvert location to the most distant point in the catchment).

The methodology presented above for determining the design flow uses several charts to calculate coefficient values. However, another method to undertake the design using these charts is to represent them mathematically. Environment Waikato (2006) derived equations to determine some of the TM61 coefficients so that spreadsheets could be developed which require minimum inputs. Environment Waikato (2006) does state however, that these equations should always be roughly checked against the charts to ensure accuracy.

There is some disagreement with the upper catchment size limit specified. Both the Ministry of Works and Development (1980) and Griffiths and McKerchar (2008) state that the upper limit is 100,000ha (1000km²). However, the Environmental Hazard Group (2012) states that the TM61 method is suitable for all catchment sizes. Ministry for the Environment (2004) indicate that the limits for the TM61 method should be 1000ha (10km²) to 100,000ha (1000km²). However, Ministry for the Environment (2004) also notes that the TM61 method also gives satisfactory results for catchments less than 1000ha. Therefore, the consensus from the literature consulted was that an upper limit of 100,000ha for the TM61 method would be the most appropriate. It should be noted that the focus of this study is on the design of single culverts, and as a result, the focus will be on smaller catchments where these are applicable. Subsequently, the catchment size limit imposed by the TM61 method will likely not be significant.

The Ministry of Works and Development (1980) indicates where the TM61 method may provide results that are not very accurate. One notable indication is the selection of a coefficient value for pumice soils. Pumice soils can be very absorbent when wet; however, after long dry periods and when the catchment is saturated, they have high runoff. Landcare Research's (2020) online soils map shows no pumice soils north of Auckland. Due to the focus area of this study being Northland, pumice soils will not have an impact. Waugh (1972), as reported by the Ministry of Works and Development (1980), gave some evidence in his publication that the TM61 method may underestimate the design discharge for smaller catchments in the Northland and Auckland regions. Waugh's (1972) evidence is an important factor to consider since the size of the catchments to be investigated will be on the smaller side while also residing in Northland.

2.5.1 Time of Concentration

The time of concentration plays a critical role in determining both design storms durations for the rational and TM61 methods. Blondelid et al. (1982) found that errors occurring during the estimation of the time of concentration could account for as much as 75% of the total error associated with the predicted peak discharge. The time of concentration is defined as the time taken for water to travel from the furthest point in the catchment to the outlet point (Environmental Hazards Group, 2012; Thomason, 2019; Department of Building and Housing, 2020). There are many different ways to calculate the time of concentration, with Ravazzani et al. (2019) reviewing 24 of the most common empirical-based methods. The Ministry of Works and Development (1980) gives four methods to calculate the time of concentration. These four methods include three equation-based ones; the Ramser-Kirpich, Bransby-Williams, U.S. Soil Conservation Service and one based on a nomogram.

The Kirpich-Ramser equation, as given by the Ministry of Works and Development (1980), is often referred to in literature as solely the Kirpich equation. The reference to Ramser is to acknowledge the work he performed developing the equation initially in 1927 before it was revised by Kirpich in 1940. Kirpich, in 1940, calibrated the equation using small agricultural catchments in Tennessee and Pennsylvania (Ravazzani et al., 2019). The Ramser-Kirpich equation follows as equation 7:

$$T_c = 0.0195L^{0.77}S_a^{-0.385} \quad (7)$$

Where,

T_c is the time of concentration in minutes.

L is the flow length from the furthest point in the catchment in meters.

S_a is the average channel slope in m/m.

To calibrate the Ramser-Kirpich equation, Kirpich studied catchments ranging in size from 0.4 to 40 ha (0.004 to 0.45 km²) with slopes from 3-12% (Fang et al., 2008; Ravazzani et al., 2019). One notable limitation expressed by Greer et al. (2018), referencing Kirpich's original publication in 1940, is that the equation should be limited to watersheds with drainage areas less than 80ha (0.8km²) and flow lengths less than 3,048 meters (10,000 feet). The limitation stated by Greer et al. (2018) was not repeated elsewhere in the literature consulted. Fang et al. (2008) and Ravazzani et al. (2019) both performed comprehensive investigations into the different methods of working out time of concentration, including Kirpich's, and neither repeated the same limitations as Greer et al. (2018). It is felt that due to the limitations stated by Greer et al. being so definitive that they would have been mentioned elsewhere in literature. As such, the limitations given by Greer et al. (2018) will be kept in mind, but for practical purposes, will be ignored.

The flow length L given in equation 7 is a point of contention, with it being interpreted in one of two ways. The first interpretation is that this flow length relates to the "flow length of the waterway in the catchment" (R. Visser, personal communication, 24th August 2021). Using the above definition, the second interpretation is that the flow length is the length from the furthest flow point in the catchment to its outlet. The second interpretation will be used in this study, and the flow length will be taken as the longest flow path of the catchment.

The Bransby-Williams equation was developed from flood discharge observations in Indian rural catchments (Ravazzani et al., 2019). The equation was first published in 1922, with the equation being

derived from catchments with drainage areas less than 13,000ha (130 km²) (Fang et al., 2008). The Bransby-Williams equation follows as equation 8:

$$T_c = \frac{0.953L^{1.2}}{A^{0.1}H^{0.2}} \quad (8)$$

Where,

T_c = time of concentration, in hours.

L = maximum flow length in km.

A = Catchment area in km².

H = the difference in elevation between the highest and lowest points along the flow path in m.

The U.S. Soil Conservation Service equation presented in the Ministry of Works and Development (1980) TM61 handbook was the most difficult of the three equation-based methods to find appropriate literature for. The difficulty finding literature for this equation was due to different names being used for it than what was stated in the handbook. The first reference to an equation representing the one stated in the handbook found was from the design of small dams (United States Bureau of Reclamation., 1987). The equation present here was not identical due to not being in SI units. Fang et al. (2005) presented the equation in their literature review and noted that the equation is essentially the Kirpich formula, and it was developed from small mountainous basins in California. The equation as it is presented in the TM61 handbook is referred to in literature as the Pickering equation (Mata-Lima et al., 2007). The U.S. Soil Conservation Service (Pickering) equation follows as equation 9:

$$T_c = \left(\frac{0.87L^3}{H}\right)^{0.385} \quad (9)$$

Where,

T_c = the time of concentration, in hours.

L = maximum flow length, in km.

H = the difference in elevation between the highest and lowest points along the flow path in m.

There is a significant amount of literature that evaluates the accuracy of empirical methods which determine the time of concentration. Ravazzani et al. (2019) found that from the 24 empirical methods evaluated that the Bransby-Williams performed the best. Comparatively, Ravazzani et al. (2019) found that while Kirpich's method did not perform the worst, it did considerably less well than the Bransby-Williams method. Azizian (2019) evaluated 36 empirical methods and ranked them on how well they performed for several goodness of fit indices. The better the fit to the indices, the lower the methods were ranked. Azizian (2019) found that Pickering (U.S. Soil Conservation Service), Kirpich, and Bransby-Williams equations ranked 2nd, 4th and 32nd out of 36 places, respectively.

The differences identified in the above studies highlights variability in the performance of the methods across different scenarios. A methodology proposed by Environmental Hazard Group (2012) would potentially limit the variability associated with the three equations and allow a more representative value to be identified and used. Environmental Hazard Group (2012) recommends that at least three methods should be used to calculate the time of concentration, with the final value being selected based on the closest two calculated values. However, The Ministry of Works and Development (1980) state that the chosen time of concentration value should be the most reasonable for the catchment and not derived by simply averaging the methods presented to calculate it.

One notable comparison made between the three empirical equations presented by the Ministry of Works and Development (1980) is that they were all developed outside New Zealand. Two were developed in North America and another in India. Empirical equations are determined from observations and experiences rather than theoretical means. Subsequently, it is thought that the three empirical methods of determining the time of concentration could potentially not be as effective as a similar method developed in New Zealand. Gericke & Smithers (2014) reinforces this thought highlighting that empirically-based coefficients represent regional effects, and subsequent use outside the calibrated catchments must be limited. There is a lack of literature evaluating these three empirical methods of determining the time of concentration in New Zealand's environment. The most relevant reference to an evaluation of these three empirical methods presented in the TM61 handbook was Griffiths & McKerchar (2012), who didn't actually evaluate them at all. Instead, Griffiths & McKerchar (2012) overlooked the three methods and instead chose to modify an existing formula and calibrate it for New Zealand conditions.

The purpose of calculating the time of concentration is to determine the design storm for the associated catchment. The design storm is derived from the rainfall intensity and depth tables presented on the NIWA HIRDS website. One key issue with these tables is that they have a minimum time of ten minutes. Costley (2018) identified this problem and the fact that the time of concentration was often less than 10 minutes for smaller catchments. The method employed by Costley (2018) to deal with this issue was to use the values given for a time of 10 minutes for any time of concentration values which were calculated to be less than 10 minutes. Thomason (2019) presents a similar methodology to Costley (2018), stating if the computed time of concentration is less than 10 minutes, then 10 minutes should be used in the subsequent rainfall intensity calculations.

2.6 Regional

The regional method has been developed from a network of river gauging stations. The observed flood records were fitted to an extreme value distribution allowing the extrapolation of flood flows for catchments for which no records exist. Regional methods are best suited for rivers from catchments exceeding 1000ha. However, regional methods can be used on catchments of 500ha or more with moderate confidence (NZFOA, 2020). The regional method is available as an interactive tool from NIWA and details New Zealand rivers' flood statistics (NIWA, 2019).

3. Objectives

This study's primary purpose is to develop tools within the ArcGIS environment using appropriate methodology to semi-automate the flood flow calculation and culvert design processes. The semi-automated design process aims to streamline existing workflows and save designers time while providing consistent and accurate results. Both the rational and Technical Memorandum 61 methods for determining the design flow will be used. At least thirty catchments of varying sizes will be evaluated across the Northland region. The catchments will be evaluated using both the new semi-automated design process and existing manual methods. The use of both these evaluation methods has the purpose of allowing results to be reconciled, discussed and their respective design times recorded.

A secondary aim of this study is to improve the design process around the selection of the rational runoff coefficient and time of concentration equations. It is also hoped that the information and analysis undertaken enhances the understanding of these processes and their impact on culvert design.

4. Methodology

The methodology used is a mixture of existing techniques and techniques developed inside the GIS environment. Both will be explained in detail in the following sections for the flood flow methods (rational and TM61) and culvert calculations.

An annual exceedance probability of 5% will be used across all catchments as the culverts' design specification. The use of this annual exceedance probability ensures that the culverts' design meets regulation 46(1) clause b of the NES-PF.

The catchments selected for the design process will be based on existing structures built by industry to ensure the relevance of the results generated. Google Earth historical imagery will be used alongside a streamflow map to locate where existing forest roads cut across a waterway. The point where the road crosses the watercourse is the assumed location of the existing structures built by industry, and these points will be used to generate the catchments required for this study.

Costley (2018) found through a phone survey that the largest typical catchment size forest employees were involved in designing were 400ha (4km²) or less. As a result, a focus will be put on evaluating catchments that fall within this area limit. The literature review undertaken identified that the rational method should only be used up to catchments of 120ha in size. For catchments above this size, the rational method will still be used, but the limitation will be noted alongside any design values specified.

Each outlet point's coordinates will be recorded alongside the other data to ensure that the catchment could be found again and redesigned. The design data developed using ArcGIS will be exported to a table as one of the process's final outputs. The data will then be saved alongside the data gathered by performing the design process manually, allowing the results to be easily interpreted and discussed.

4.1 Software and Data Sources

The Global Information Software (GIS) used to semi-automate the design process will be ArcMap 10.8.1. ArcMap can automate processes through a model builder and the use of scripts developed with python. A mixture of these two methods will be used to automate the process as much as practical and to minimise the inputs and interaction with the model. The model could potentially require reasonable processing time. However, the model will not need supervision, so it can be left to run in the background while the user undertakes other tasks.

A digital elevation model with a grid size of 1x1m will be developed from LiDAR data for the Northland region. The LiDAR data was sourced from the local council as a series of tiff images. The images required further processing to turn them into a single layer to allow easy analysis. The conversion of multiple images into a single layer was undertaken using ArcMaps mosaic to new raster tool.

The Land Resource Information System (LRIS) portal was used to obtain the latest Land Cover Data Base (LCDB) of New Zealand. The fifth LCDB version is used in the analysis, with the data dated 2018/19 of key interest. The soil drainage map provided on soils map viewer was used to classify the soils for both the rational and TM61 methods. The data used in the online map was obtained through the LRIS portal also and is called the FSL Soil Drainage Class. It is noted that the FSL layer is mapped at a 1:50000 scale which subsequently affects its accuracy. There is another map called S-Map Soil Drainage, which provides a more comprehensive and up to date source of soil data. However, the coverage of this map is limited, and the

layer does not yet cover Northland. Therefore, the FSL layer will be used in the analysis. The key used to classify the different soil layers follows in figure 8.

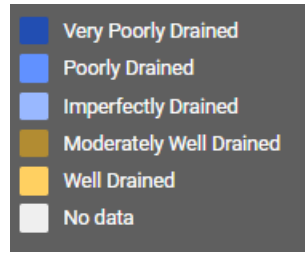


Fig 8. Drainage key for soil layer.

McCormack’s (2020) classification system to identify the relevant TM61 soil type will be used and adapted with a similar classification pertaining to the rational method specified. Table 3 follows and gives the classification method used.

Table 3. McCormack’s (2020) classification system for soils relating to the TM61 method adapted to include the rational method.

Landcare Research Classification	TM61 Classification	Rational Classification
Very poorly drained	Impervious soils	Heavy Clay
Poorly drained	Impervious soils	Heavy Clay
Imperfectly drained	Moderately absorbent soils	Medium Soakage
Moderately well-drained	Moderately absorbent soils	Medium Soakage
Well-drained	Absorbent soils	High Soakage

4.2 Rational Method

Semi-Automated Process

The model created to help semi-automate the rational method’s design process is split into three distinct parts. These three parts include analysis of the catchment, runoff coefficient derivation and final calculations. The first part of the model takes a given outlet point (location of culvert), a digital elevation model, a snap-pour-point distance and a file name. The outputs generated from these four inputs include the catchment area, the longest flow path, the maximum and minimum elevation points and the average slope along the flow path. The user interface of the first part of the model follows in figure 9.

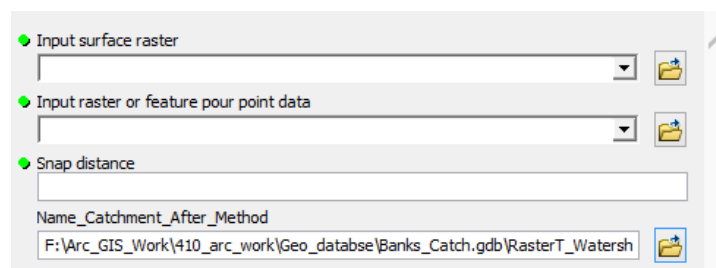


Fig 9. Tool interface, which performs analysis of catchment (step 1 of the process).

From figure 9, the four inputs mentioned above can be easily identified. The input surface raster relates to the digital elevation model, the feature pour point data relates to the culvert location and the snap distance to snap-pour-point distance. The use of the snap distance is to reduce incorrect catchments being built from the culvert location. The tool snaps the point of interest a specified distance to the largest flow path nearby, ensuring the catchment of interest is created. Finding the snapping distance can be an iterative process and must be conducted with a degree of caution. Typically around a 10m snapping distance will provide the necessary results. However, the catchment generated needs to be investigated to ensure it is still representative of what is required (location of the outlet hasn't moved too far). The tool uses both ArcMap's in-app model builder and a python script to perform the required functionality. Figure 10 follows and displays the tools and processes used to semi-automate the analysis of a catchment.

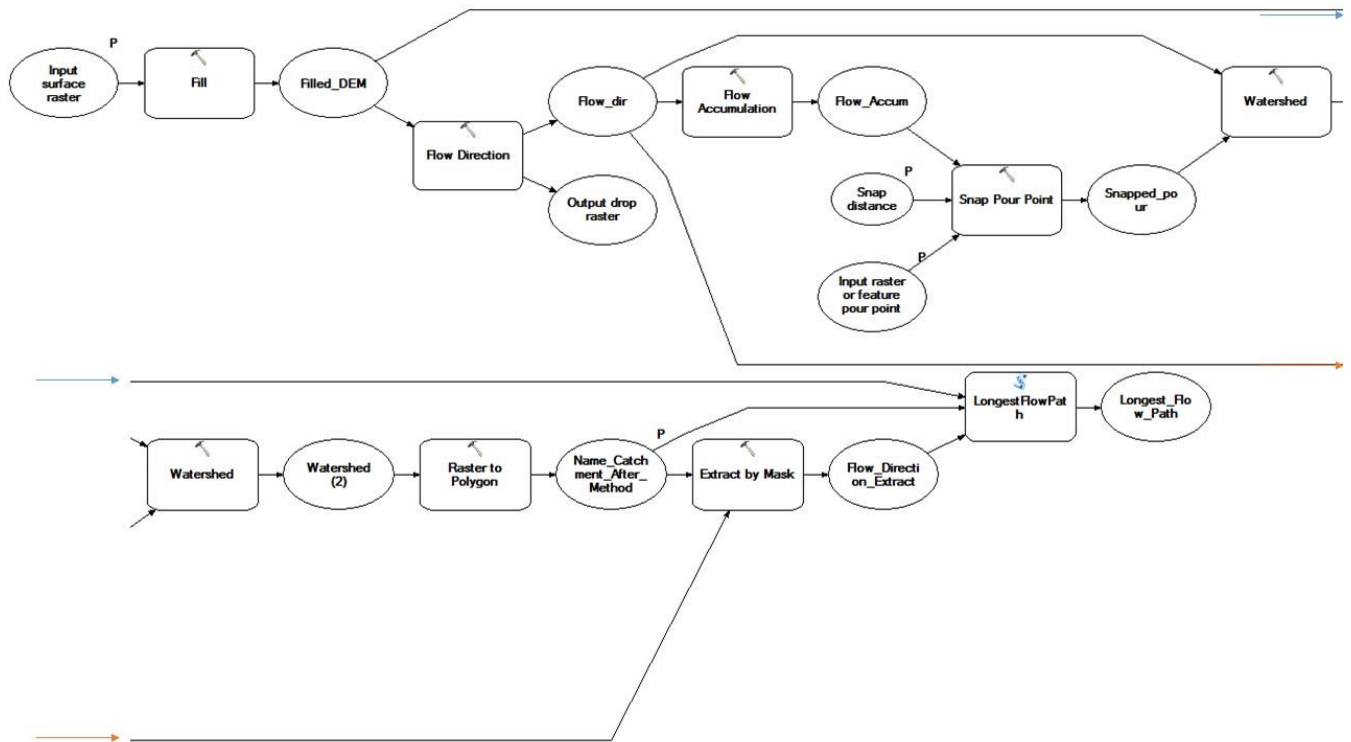


Fig 10. A model builder screen clipping of the tools used in the analysis of the catchment.

From figure 10, the script can be seen as the last tool utilised and is named the longest flow path. The script was sourced from an ESRI discussion forum and was published by Sturtevant (2017). The script Sturtevant developed uses raster statistic methods and cost-path analysis to find the longest flow path. The script was then altered to calculate the required characteristics of the flow path. The required characteristics included the change in elevation and average slope of the flow path. The add surface information tool was used to work out the required characteristics. The script used to produce the flow path and the required characteristics is in appendix a.

The runoff coefficient derivation tool is broken into two substeps, with the first being a supervised classification. The Land Cover Data Base (LCDB) is clipped to the catchment of interest and then reclassified into the rational land classes shown below in table 4. The rational land classes are based on figure 4.

Table 4. LCDB alongside their respective Rational Land Classes and runoff values.

Land Class LCDB	Rational Land Class	Rational Runoff Value	Land Class LCDB	Rational Land Class	Rational Runoff Value
Not Land	N/A	No Data	Tussock Grassland	Pasture and grass cover	0.3
Built up	Fully roofed and/or sealed developments	0.9	Depleted Grassland	Pasture and grass cover	0.3
Urban Park	Parks, playgrounds and reserves mainly grass	0.3	Herbaceous Freshwater	N/A	No Data
Transport Inf	Asphalt and concrete surface	0.85	Herbaceous Saline	N/A	No Data
Mines&Dumps	Bare Soil	0.5	Flaxland	Bush and Scrub Cover	0.25
Sand&Gravel	Bare Soil	0.5	Fernland	Bush and Scrub Cover	0.25
Landslide	Bare Soil	0.5	Gorse&Broom	Bush and Scrub Cover	0.25
Snow&Ice	N/A	No Data	Manuka&Kanuka	Bush and Scrub Cover	0.25
Alpine Grass	Pasture and grass cover	0.3	Broadleaved Indig	Bush and Scrub Cover	0.25
Gravel&Rock	Unsealed Roads	0.5	Sub Alpine Shrubland	Bush and Scrub Cover	0.25
Lake&Pond	N/A	No Data	Mixed Exotic Shrubland	Bush and Scrub Cover	0.25
River	N/A	No Data	Grey Scrub	Bush and Scrub Cover	0.25
Estuarine	N/A	No Data	Forest Harvested	Harvested	0.5
Cropland	Pasture and grass cover	0.3	Deciduous Hardwood	Bush and Scrub Cover	0.25
Orchard&Vineyard	Bush and Scrub Cover	0.25	Indigenous Forest	Bush and Scrub Cover	0.25
High Producing Grass	Pasture and grass cover	0.3	Mangrove	Bush and Scrub Cover	0.25
Low Producing Grass	Pasture and grass cover	0.3	Exotic Forest	Exotic Forest	0.25

The rational runoff values presented above in Table 4 have been altered where the soil drainage directly influenced them. The values in the table above also do not account for the effects of slope. The classification scheme used in table 5 accounts for both the effects of slope and soil drainage. Table 5 summarises the corrective data applied to the C factor with the soil classification given in table 3 and numeric C factor corrections for both soil and slope provided in figures 3 and 4.

Table 5. Rational method classification scheme for the soil drainage and slope effects.

Soil Drainage Class	Rational Equivalent	C Alteration	Slope Threshold (%)	C Alteration
Very Poorly Drained	Heavy Clay	+ 0.2	< 5	- 0.05
Poorly Drained			5 - 10	0
Imperfectly Drained	Medium Soakage Types	+ 0.1	10 - 20	+ 0.05
Moderately Well Drained			> 20	+ 0.10
Well Drained	High Soakage	+ 0		

With the LCDB values reclassified into their rational equivalents, a reality check needs to be made on the land cover of the catchment. The data for the LCDB is from the year 2018/2019, and as such, the land cover across the catchment could have changed since the layer was developed. However, it is assumed that the changes in land cover that have occurred will primarily relate to plantation forests. The changes which have occurred in plantation forests within the catchment will be investigated using Google Earth, and the layer will be edited manually to update any significant changes observed. The manual editing that occurs can also be used to detail where a planned harvest is proposed allowing a more representative runoff coefficient to be developed. The editing step is the last part of the manual classification step.

The second step combines the three sets of data; the reclassified land cover database, the soil drainage layer and a slope map into a single runoff coefficient value using the values given in tables 4 and 5. The ArcMap processes used for each of the two steps explained above follow, and screenshots of the processes can be found in Appendix B.

First step:

- Clip LCDB to the extent of the catchment.
- Add field to clipped LCDB layer and reclassify into rational land cover classes using a script and the field calculator.
- Manually inspect and update land cover values relating to harvested land and exotic forests where required.
- Output = reclassified LCDB shapefile that represents the catchment.

Second step:

- Inputs into tool include; LCDB reclassified, Digital Elevation Model (DEM), Catchment polygon and soil drainage map.
- Add a new field to reclassified LCDB layer and add the rational runoff values from table 4 using a script and the field calculator.
- Use extract by mask tool to clip the DEM to the catchment.

- Use the tool clip to do the same to the soil drainage map using the catchment polygon.
- Clipped DEM:
 - Fill it to remove sinks.
 - Use slope tool in per cent with a cell size of 1x1m.
 - Reclassify using table 5 values to give slopes contribution to runoff coefficient.
- Combine both the soil drainage map and reclassified LCDB using the intersect tool.
- Add a new field to the resultant table based on both the LCDB and soil drainage characteristics. The new field will have C values denoted to it based on the corrections for soil drainage from table 5. The field will only have values for the land covers, which need a correction applied for soil type, i.e. pasture and bush. If the land cover does not need to be corrected for soil drainage, i.e., Asphalt, 0 will be assigned to this field.
- Add another new field to the table and combine the corrective soil factors and LCDB runoff values using the field calculator.
- Convert the layer to a raster based on the combined soil and LCDB runoff value. Set cell size to 1x1m.
- Combine the LCDB and soil raster with the slope raster to produce a final runoff coefficient raster using the raster calculator tool. For this raster, each cell (1x1m) now has a unique associated runoff coefficient.
- Use the zonal statistics as table tool to generate the average runoff coefficient (like equation 3). The average runoff coefficient generated here is what will be used in the culvert design process stage.

The final calculations tool brings all the data together and gives a table of results, including the size of the required culvert. The inputs required to this tool include; the catchment area, runoff coefficient value, longest channel length, average channel slope, minimum and maximum elevation along the channel, the selected time of concentration equation, the path to the comma separated value (CSV) file for the rainfall data and culvert parameter selection. The inputs provided are gathered in the python environment using the get parameters as text function. In the python environment, the inputs are used to determine the time of concentration, rainfall intensity, peak design flow, and culvert sizing. The final step before the script completes is to produce a summary table of all the inputted and calculated values of interest for the specified catchment.

The user specifies which time of concentration equation they would like to design with. The tool can then be re-run multiple times to generate a table of results for each time of concentration equation. The equations used to calculate the time of the concentration are 7, 8 and 9.

The rainfall data is acquired from NIWA's High Intensity Rainfall Design System V4. The NIWA tool generates a rainfall report based on given coordinates. The report is then available for download in a CSV format. The CSV report has a singular structure, and as a result, the required values can be extracted using arrays. An equation is given in the NIWA report, which allows a rainfall intensity to be calculated for any given time of concentration. The equation will be used alongside the extracted values to determine the required rainfall intensity associated with the catchment.

Manual Process Rational

In conjunction with the semi-automated process, the catchment will also be designed manually. The manual design process used will be similar in some parts to Costleys (2018), McCormacks (2020) and the

semi-automated one presented above. The steps undertaken to perform the manual design procedure follow:

- Catchment area found using a contour map and DEM within ArcMap.
- Longest stream path used to create an elevation profile.
 - Points generated at 5m intervals along the longest flow path, including the start and end points using the generate points along lines tool.
 - Elevation data added to each of the points along the line using the add surface information tool.
 - Export the attribute data in CSV format.
 - In excel, add the horizontal points (start at 0m and add 5m for every elevation point).
 - Find the minimum and maximum elevation points and the length of the flow path from the excel data.
 - Plot the elevation data against the horizontal points to produce an elevation profile.
 - Average slope calculated through the equal area method. The equal area method is shown below in figure 11.
- Runoff coefficient determined using figures 4, 5 and table 3.
 - ArcMap aerial imagery base map used to determine land cover proportions. Google Earth used as a reality check.
 - The average catchment slope will be used to apply the slope correction factor.
 - The soil type with the largest area in each land cover chosen to be fully representative for that land cover. Soil corrective factor then applied.
 - Weighted runoff coefficient will then be determined using equation 3.
- The time of concentration will be calculated with equations 7, 8 and 9.
- Intensity determined using the NIWA HIRDS rainfall data.
- Culvert sizing will be undertaken with the charts presented in figures 1 and 2.

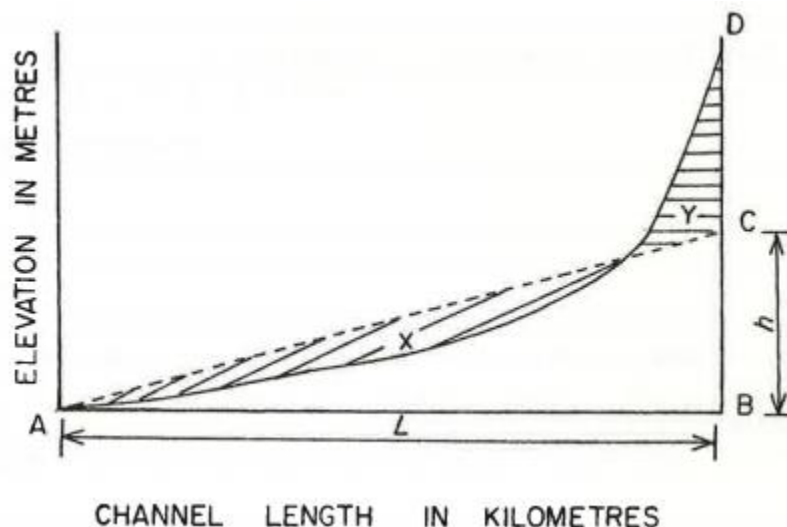


Fig 11. The equal area method for determining average channel slope.

4.3 TM61

Semi-Automated

The model created to help semi-automate the TM61 design process comprises of three parts. These three parts include analysis of the catchment, cover coefficient classification and final calculations. The catchment analysis uses the same process as the rational method, so it will not be repeated.

The cover coefficient (W_{IC}) will be partially automated with the proportions of land and soil cover determined, but a numeric value will not be assigned. Like the rational runoff coefficient classification step, the process is broken into two sub-steps, with the first being a supervised classification. The Land Cover Data Base (LCDB) is clipped to the catchment of interest and then reclassified into the TM61 land classes shown below in table 6. The TM61 land classes are based on figure 12. The process used in ArcMap is the same as the first step (bar the different land cover classifications) of the runoff coefficient tool for the rational method and subsequently won't be repeated.

Table 6. LCDB land classes and their corresponding TM61 land classes.

Land Class LCDB	TM61 Land Class	Land Class LCDB	TM61 Class
Not Land	NoData	Tussock Grassland	Long grass, scrub or bush
Built-up	NoData	Depleted Grassland	Short grazed
Urban Park	NoData	Herbaceous Freshwater	NoData
Transport Inf	Bare Surfaces	Herbaceous Saline	NoData
Mines&Dumps	Bare Surfaces	Flaxland	Long grass, scrub or bush
Sand&Gravel	Bare Surfaces	Fernland	Long grass, scrub or bush
Landslide	Bare Surfaces	Gorse&Broom	Long grass, scrub or bush
Snow&Ice	NoData	Manuka&Kanuka	Long grass, scrub or bush
Alpine Grass	Long grass, scrub or bush	Broadleaved Indig	Long grass, scrub or bush
Gravel&Rock	Bare Surfaces	Sub Alpine Shrubland	Long grass, scrub or bush
Lake&Pond	NoData	Mixed Exotic Shrubland	Long grass, scrub or bush
River	NoData	Grey Scrub	Long grass, scrub or bush
Estuarine	NoData	Forest Harvested	Bare Surfaces
Cropland	Short grazed	Deciduous Hardwood	Long grass, scrub or bush
Orchard&Vineyard	Long grass, scrub or bush	Indigenous Forest	Long grass, scrub or bush
High Producing Grass	Short grazed	Mangrove	Long grass, scrub or bush
Low Producing Grass	Short grazed	Exotic Forest	Exotic Forest

Soils	Ground Surface-Cover		W _{IC}
Impervious soils (such as clay soils with poor structure e.g. northern yellow brown earths). Any soil, if saturated, is included in this group.	Urban Catchments	high density development	1.6
		moderate to low density development	1.5
	Mainly bare surfaces		1.2
	Average shortgrazed catchments		1.1
	30% of area in long grass, scrub or bush		1.0
	60% of area in long grass, scrub or bush		0.9
	100% of area in long grass, scrub or bush		0.8
Moderately absorbent soils (such as medium textured soils with good structure e.g. southern yellow brown earths).	Urban Catchments	high density development	1.7
		moderate to low density development	1.3
	Mainly bare surfaces		1.1
	Average shortgrazed catchments		1.0
	30% of area in long grass, scrub or bush		0.9
	60% of area in long grass, scrub or bush		0.8
	100% of area in long grass, scrub or bush		0.7
Absorbent soil (such as deep yellow brown sands and pumice soils).	Urban Catchments	high density development	1.5
		moderate to low density development	1.2
	Mainly bare surfaces		1.0
	Average shortgrazed catchments		0.9
	30% of area in long grass, scrub or bush		0.8
	60% of area in long grass, scrub or bush		0.7
	100% of area in long grass, scrub or bush		0.6
Very absorbent pumice soil.	Mainly bare surfaces		0.5
	Average shortgrazed catchments		0.5
	30% of area in long grass, scrub or bush		0.4
	60% of area in long grass, scrub or bush		0.4

Fig 12. TM61 W_{IC} coefficient values (Ministry of Works and Development, 1980).

The reclassified LCDB layer can then be interacted with and altered to represent the effects of harvesting in the catchment. Alongside incorporating the effects of harvesting, manual editing also has the purpose of updating any significant changes in land cover (relating to plantation forestry) within the catchment. With any changes made to the reclassified LCDB layer saved, the second step in the classification can be undertaken. The second step works out the proportion of land covers pertaining to a given soil type in the catchment.

- Inputs into the tool include; LCDB reclassified layer, Catchment polygon and FSL soil drainage map.
- Use the tool clip to clip the FSL soil drainage map using the catchment polygon.
- Add a new field to the FSL layer and classify it based on the drainage classification system given in table 3 above.
- Combine both the reclassified soil drainage map and LCDB layers using the intersect tool.
- Add a new field and check using logic what soil drainage property and land cover coincides with an area – create classes that are identical to figure 12, i.e. Impervious Soil and Short grazed.
- Combine all the similar polygons using the dissolve tool. Now have the total area of the catchment relating to each specific soil and land cover.
- Add a new field and calculate the proportion that these specific areas make up.
- Use the proportions generated to help choose a value for the cover coefficient (W_{IC}) from figure 12.

The final calculation will be undertaken again using a script and equations developed by Environment Waikato (2006) for some of the nomograms and charts presented in the TM61 handbook. Equations 10, 11, 12a and b are taken from Environment Waikato (2006). Environment Waikato (2006) state that these equations should always be checked against the figure to ensure accuracy. Due to the design process being undertaken manually, the results of the equations will be checked automatically. A direct comparison can then be made between the measured and equation-based values. The inputs into the script include; the cover coefficient (W_{ic}), the catchment area, the direct length, the longest flow path distance, the average slope of this flow path, the maximum and minimum elevation points along the flow path, the selected time of concentration equation, the path to the CSV file for the rainfall data and a choice of the design culvert wanted.

The slope coefficient and discharge coefficient are the first values to be calculated in the script. They are calculated using equations 10 and 11, which follow.

$$W_s = 18.82S_a^{0.33}L^{0.368} \quad (10)$$

Where,

- W_s is the slope coefficient
- S_a is the average channel slope (%)
- L is the maximum channel length (km)

$$C = 0.42(W_s W_{ic})^2 \quad (11)$$

Where,

- C is the discharge coefficient
- W_s the slope coefficient
- W_{ic} the cover coefficient

The time of concentration will be calculated using the same way as the rational method. The resulting design intensity will be then converted into design rainfall depth. The rainfall factor, given by equation 5, is the ratio of the design rainfall depth and standard rainfall depth. The standard rainfall depth is calculated using equation 12a or 12b depending on the time of concentration. Equation 12 a and b follow:

$$R_{sd} = 13.197d^{0.4274} \quad \text{For } 10\text{mins} < D < 120\text{mins} \quad (12a)$$

$$R_{sd} = 9e^{-8d^2} - 0.0003d^2 + 0.5363d + 43.2 \quad \text{For } 120\text{mins} < D < 24\text{hrs} \quad (12b)$$

Where,

- R_{sd} is the standard rainfall depth (mm)
- d is the storm duration (minutes)

The shape factor equation was derived using excel and a fifth-order polynomial trendline. The equation derivation process for the shape factor is shown below in figure 13.

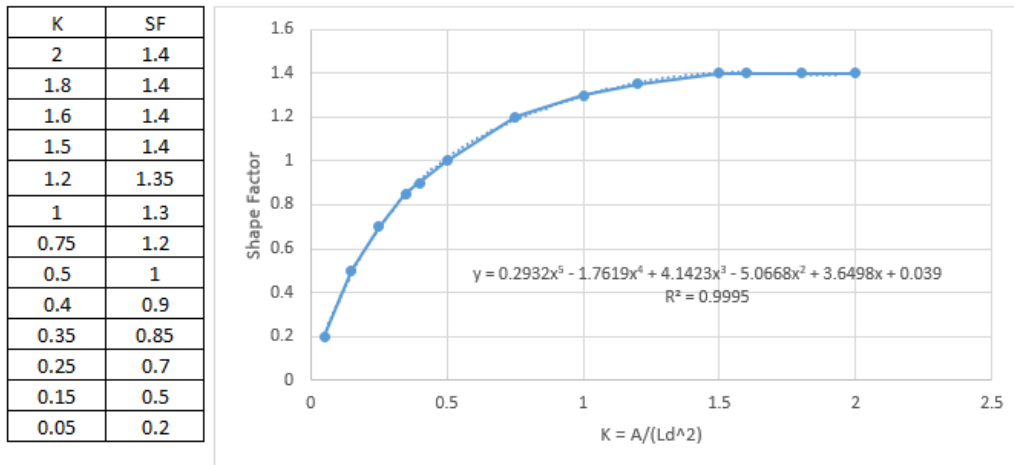


Fig 13. Equation derivation for the shape factor.

The shape factor is the last parameter required for equation 4 to produce the TM61 flood flow estimation. The culvert will then be designed using the inputted specification, and a summary table will be produced of the results. It is noted that there are different units across the number of equations used in the proposed methods. Therefore, the values to be inputted will specify what units to use, and the script will convert as required in the background.

Manual Process TM61

In conjunction with the semi-automated process, the catchment will also be designed manually. The manual design procedure is specified by the Ministry of Works and Development (1980). The exact methods used will be similar to Costleys (2018), McCormacks (2020) and the semi-automated one presented above. The first two steps are identical to those used in the rational manual process and will not be repeated. The steps undertaken after these two are as follows:

- Cover coefficient (W_{IC}) determined using figure 12 (shown above) and table 3.
 - ArcMap aerial imagery base map used to determine land cover proportions. Google Earth used as a reality check.
 - The soil type with the largest area in each land cover chosen to be fully representative for that land cover. Table 3 used to determine the soils drainage characteristics.
- The slope coefficient W_s determined using figure 14.
- Discharge coefficient (C) determined using figure 15.
- Standard rainfall depth determined using figure 16.
- The time of concentration will be calculated with equations 7, 8 and 9.
- Rainfall depth determined using the NIWA HIRDS rainfall data.
- Rainfall factor calculated using equation 5.
- Shape factor determined using figure 17.
- Estimate peak discharge using TM61 equation 4.
- Culvert sizing will be undertaken with the charts presented in figures 1 and 2.

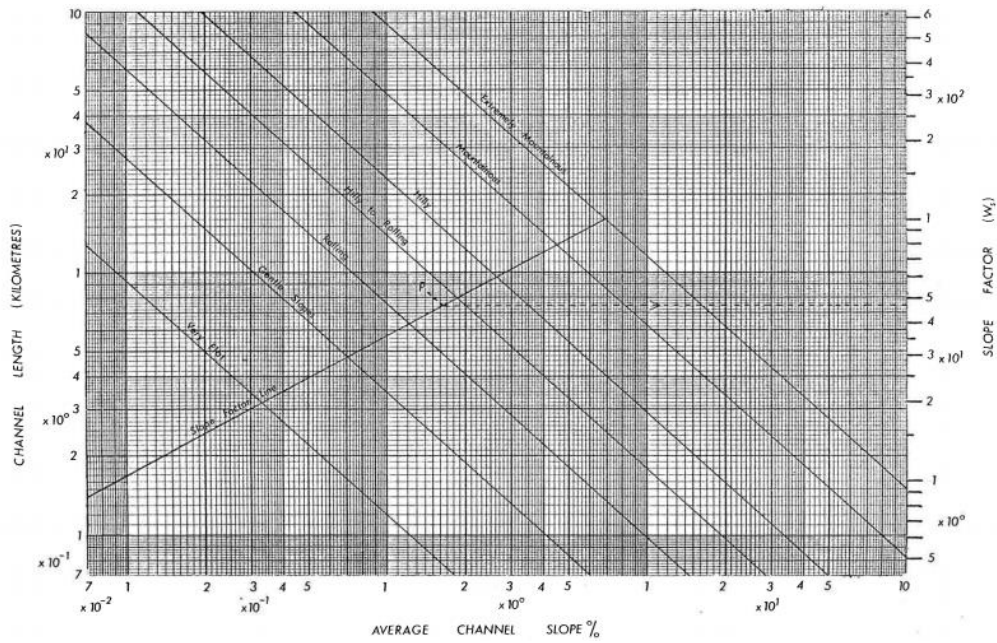


Fig 14. Chart for slope coefficient W_s .

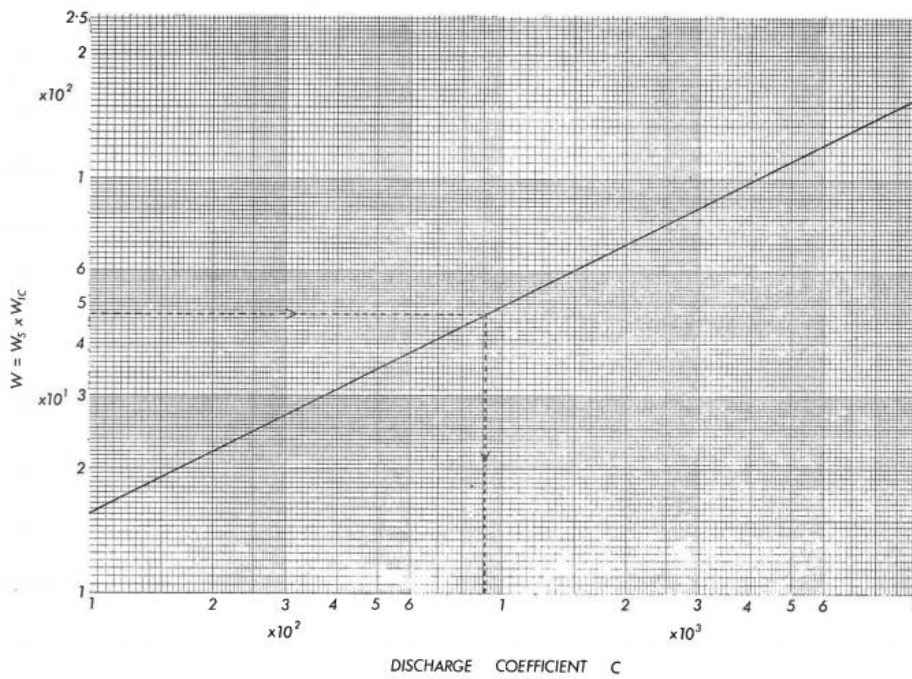


Fig 15. Chart for determining discharge coefficient C .

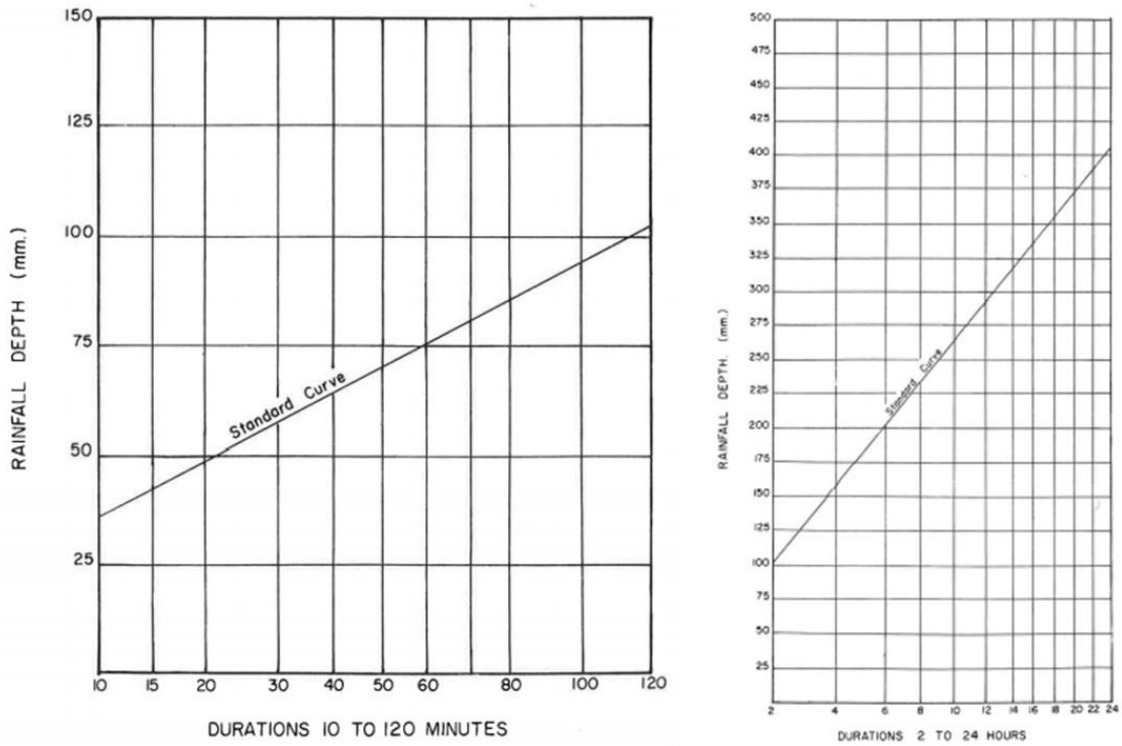


Figure 16. Chart for determining the Standard Rainfall Depth.

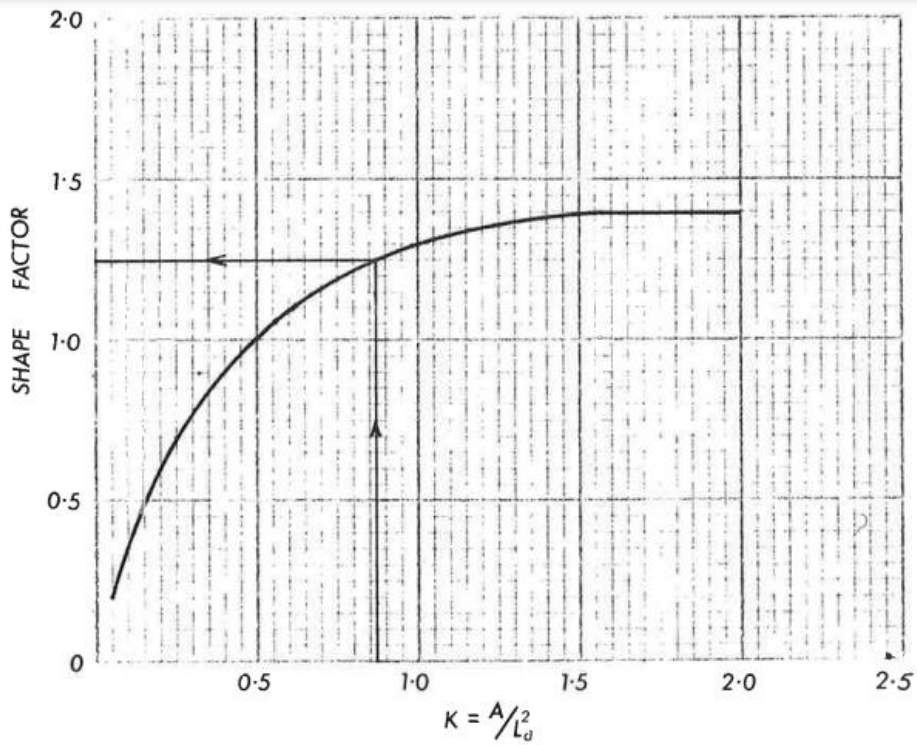


Fig 17. Chart for determining the shape factor.

Culvert Calculations

To perform the culvert sizing as part of a script, the charts presented in figures 1 and 2 needed to be replicated using equations. The process used to turn the culvert sizing charts into equations was the same as what is shown in figure 13 for the shape factor. A number of points were determined for both the design flow and corresponding culvert size. These points were then plotted with a trendline fitted to approximate them as best as possible. The creation of the equation assumes that the user follows the NES-PF guidelines of designing without allowing heading up, i.e. the heading up ratio is equal to one. If the user is not following these guidelines, the equations derived cannot be used, and the result given will not be representative of what they require. Figure 18 follows and shows this process being undertaken for a corrugated metal culvert with headwalls and wingwalls as the entrance type.

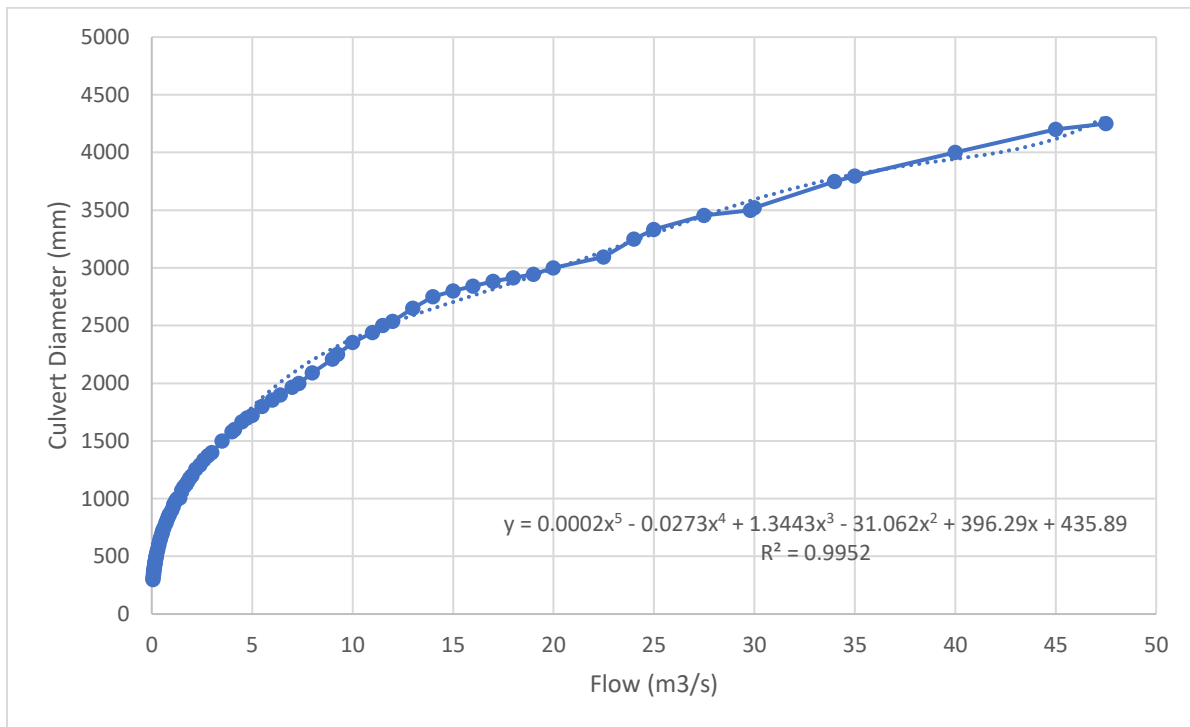


Fig 18. Example of culvert equation derivation.

Figure 18 above shows one example of an equation being derived for culvert sizing. Initially, equations were developed for the five other scenarios that the nomograms are used to calculate (different materials and entrances). However, it was decided that to test the validity of the method used to replicate the nomogram comprehensively, only the equation presented above in figure 18 would be evaluated in this study. The proposed equation representing the nomogram of a corrugated metal culvert with headwalls and wing walls as its entrance type follows as equation 13.

Corrugated metal – Headwalls and wingwalls.

$$\text{Diameter} = 0.0002x^5 - 0.0273x^4 + 1.3443x^3 - 31.062x^2 + 396.29x + 435.89 \quad r^2 = 0.9952 \quad (13)$$

Where x is the estimated flow in m³/s and diameter is the culvert diameter in mm.

5. Results and Analysis

5.1 Catchment characteristics

5.1.1 Location

In total, 35 stream crossing sites across Northland were designed. The locations of these sites are given and numbered in figure 19, which follows.



Fig 19. Location of the stream crossings designed in this study.

5.1.2 Catchment Area

The average catchment area of the 35 crossings designed was 160.7ha. Figure 20 follows and displays the area of each catchment evaluated in this study.

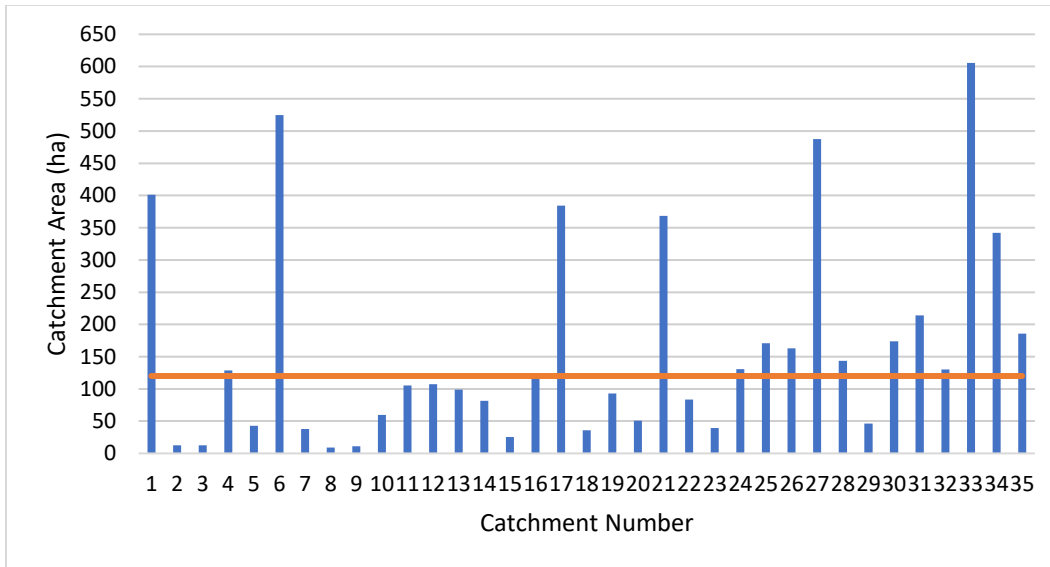


Fig 20. The sizes of the catchments that were designed.

The orange line above in figure 20 highlights the catchment size limit appropriate for designing using the rational method (120ha or less). The catchments above this line fall outside this specification. The area of each catchment designed was found using both semi-automated and manual methods. A comparison between the catchment areas recorded for both methods follows in figure 21.

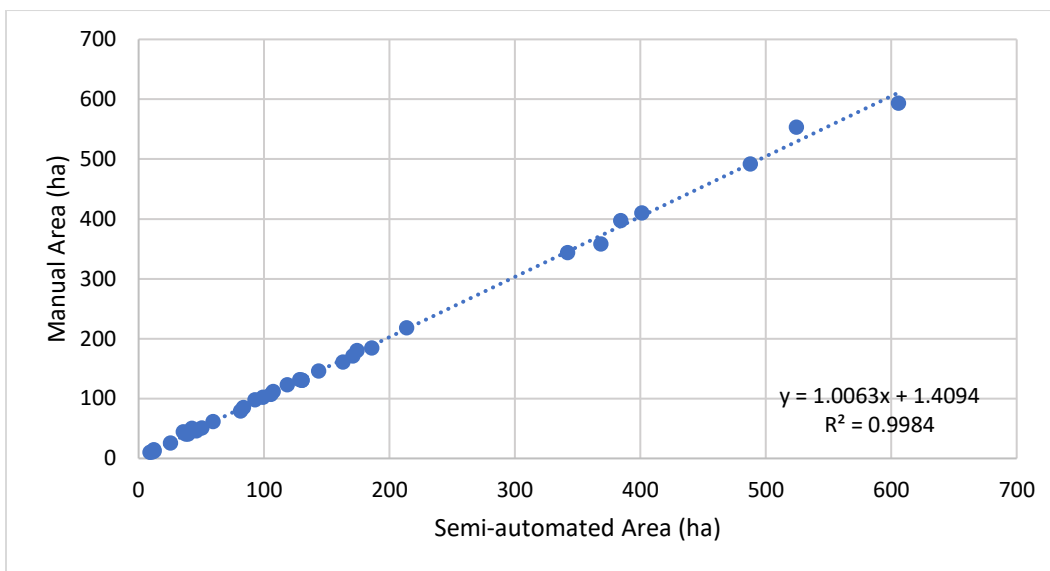


Fig 21. The catchment areas calculated using the two methods.

Figure 21 shows that the manual and semi-automated measurements of the catchment area fit the linear regression model very well ($r^2 = 0.9984$). A linear model is appropriate to portray the relationship as, in theory, the two measurements of the same variable should be equal. The equation of the linear trendline shows that x is approximately equal to y meaning the two should give identical values if the y -intercept is ignored. Comparing the difference between the two measurements of catchment area showed that the manual method produced an area that was 2.42ha larger on average. The difference in area between the

two methods can be likely attributed to the scale at which the manual area was defined and human error made during the measurement process. On occasion, the manual catchment area measurement process had to be redone due to the initial measurement overestimating the catchment size significantly. The instances where the manual process caused the significant overestimate highlighted the vulnerability of the manual measurement process to causing significant error and variability in the design.

5.1.3 Channel Slope

The average channel slope was identified as a catchment variable that differed drastically between the semi-automated and manual measurements. The manual measurement utilized the equal area method, and the semi-automated method used an inbuilt series of tools within ArcGIS to calculate the average channel slope. In addition to these two methods, an averaged points measurement of channel slope was derived from the same data used to produce the graph required for the equal area method.

The averaged points measurement of channel slope was calculated by averaging 5m increments of channel length for slope along the entire length of the channel. It was assumed that the 5m increments were small enough that this length could be taken to represent the horizontal distance required for calculating slope. It should be noted that a smaller increment is more representative of the actual horizontal distance taken. However, increments below 1m in length shouldn't be used due to the elevation data having a spatial resolution of 1m². Increments less than 1m in length would lead to increments having a slope of 0% due to both points falling within a single elevation cell, highlighting the importance of staying within the limits of the elevation data's capability.

The average points method was determined to be an overcomplicated way of finding the average slope of the stream channel. While undertaking a discussion with colleagues, it was pointed out that the average slope produced using this method is equivalent to that produced by averaging the start and end points of the channel. While overcomplicating the average channel slope measurement, the average points method does provide a logical and easy distinction between the different methods used.

Both the average points and semi-automated methods measure the average channel slope and are directly comparable. However, by definition, the equal area method provides the equal area slope and cannot be directly compared to the average slope. Although, the relationship between the average and equal area measurements is still worth observing as the two varied quite significantly while providing a measure for the same variable, the channel slope. The three measurements of channel slope and the values they produced for each catchment designed for follow in figure 22.

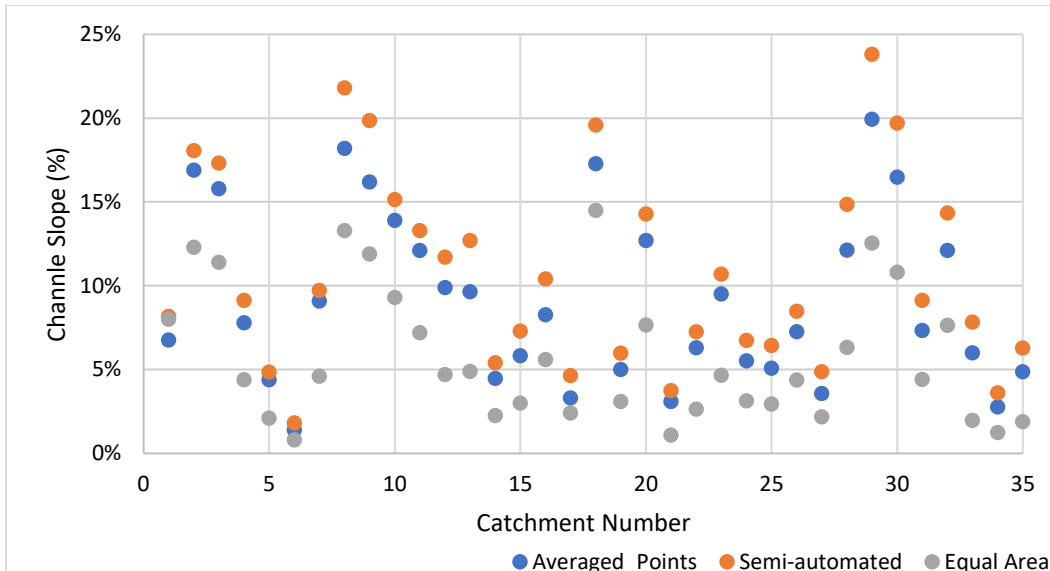


Fig 22. Comparison of the channel slope measurements.

The average points method is thought to produce a more accurate representation of the average channel slope than the semi-automated method. As a result, figure 22 highlights that the semi-automated process overestimates the average channel slope. On average, the semi-automated method produced a slope 0.017m/m (21%) larger than that produced using the average points method. The overestimation of the semi-automated process is surprising as it uses a similar methodology to the average points method. However, it is noted that the increments of channel length that the semi-automated process averages across are somewhat longer. The semi-automated process also weights the slope based on the length of the increments, which gives another potential source of variability.

Figure 22 also highlights that the equal area method produces a smaller estimate of the channel slope than the average points method. On average, the equal area method produced an estimate of channel slope 0.034m/m (41%) less than one produced using the average points method. The difference of 41% is quite substantial, and the effect it has on the flow design value calculated is significant. It is thought that while the methods differ in their approach for measuring the channel slope that the values produced should not differ by as much as they did.

The average point's method of slope determination was not explored further in the analysis as it was not one of the focal points of this study. However, the average point's method highlights a potential weakness associated with using both the equal area method (currently used in industry) and the semi-automated method developed for this study. Therefore, the average point's method highlights a potential area where further research could be conducted, i.e. which method is appropriate for determining channel slope. The difference between the slope measurements of the manual and semi-automated methods allowed the channels slope effect on flow to be investigated. The percentage difference between the channel slope measurements of each method follows in figure 23.

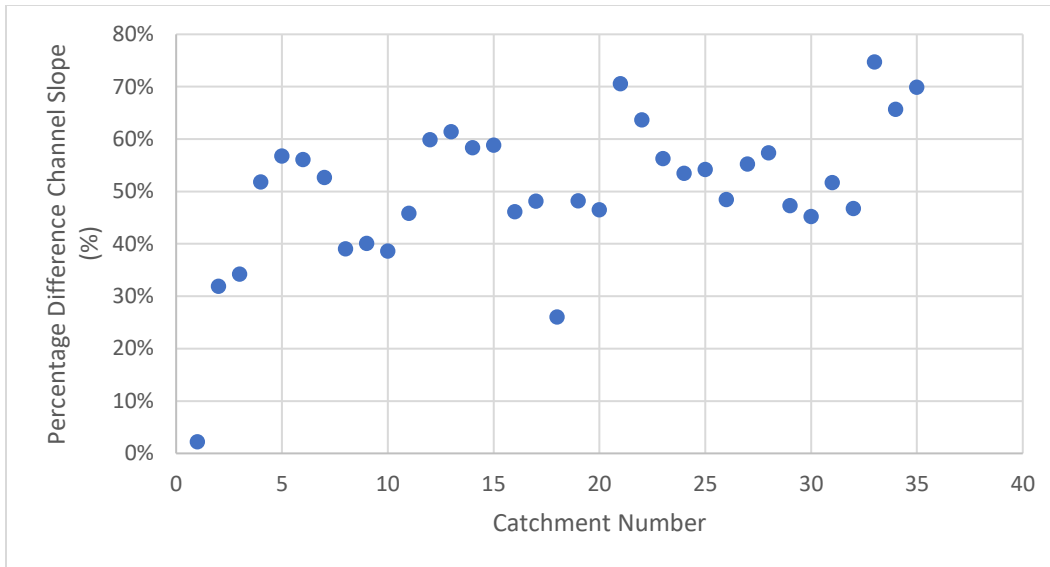


Fig 23. Percentage difference of channel slope between the semi-automated and equal area methods.

The percentage difference between the two measurements further highlights the variability between the two methods in determining channel slope. It is expected that catchment 1 is an outlier due to the spread of the other data. The average percentage difference in the channel slope between the two methods was 50.4%.

5.1.4 Channel Slope and Flow Rate

The flow calculated for each catchment was impacted to varying degrees by the differences in channel slope dependent on the methods used. The rational method employing Williams and U.S. Soil conservation time of concentration equations was not affected due to these two methods relying on the maximum and minimum elevation points along the channel instead of its slope. However, the rational method utilizing Kirpichs time of concentration equation and the TM61 method for all three time of concentration equations were both significantly impacted (see section 2.5.1 for equations). For simplicity, only the three TM61 flow comparisons will be shown in figures 24, 25 and 26.

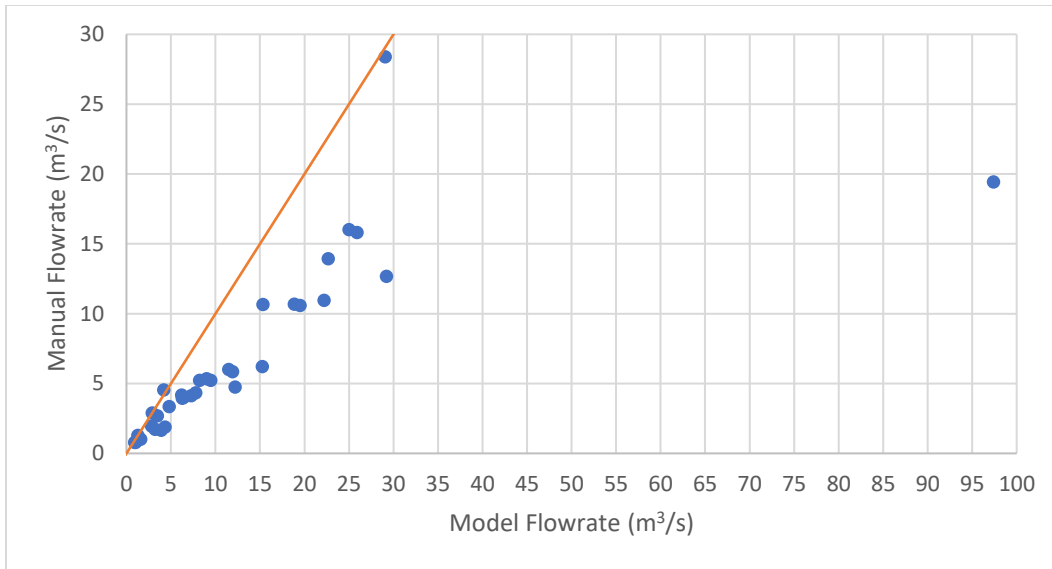


Fig 24. The manual and semi-automated flow rates using Kirpich's time of concentration equation for the TM61 method.

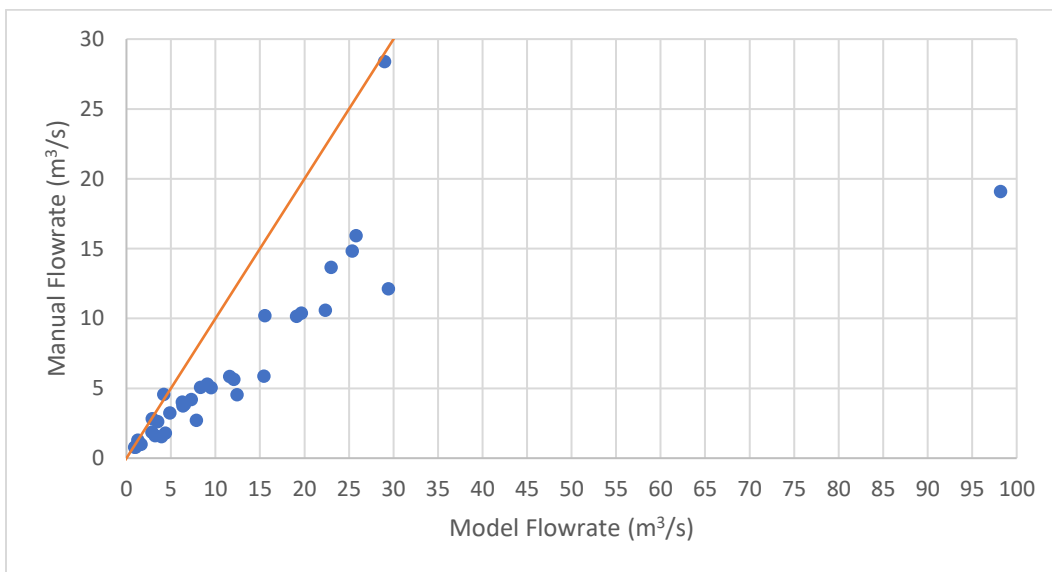


Fig 25. The manual and semi-automated flow rates using U.S. Soil Conservation time of concentration equation for the TM61 method.

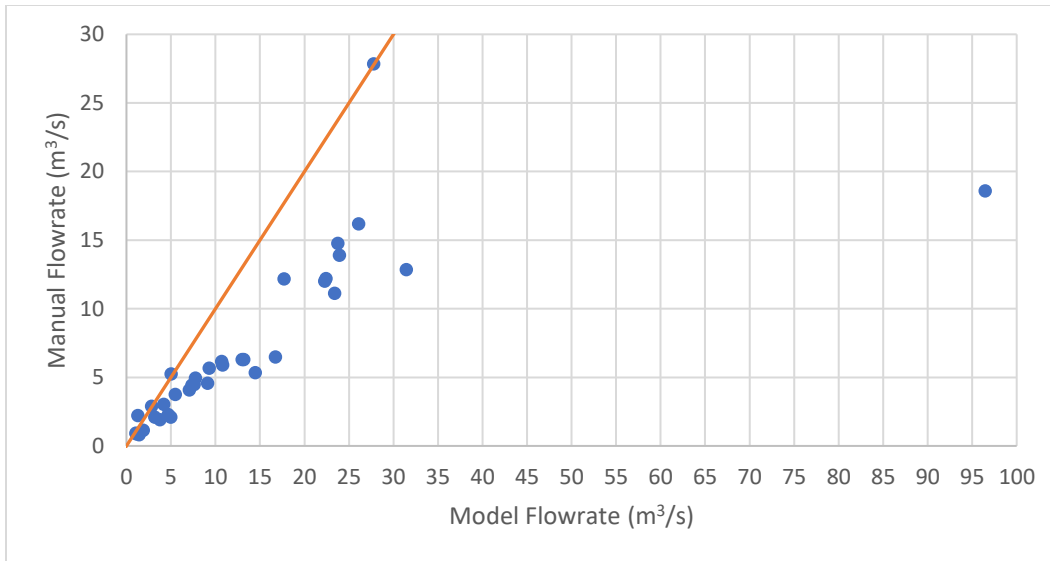


Fig 26. The manual and semi-automated flow rates using Williams time of concentration equation for the TM61 method

The orange line in figures 24, 25 and 26 indicates where the semi-automated and manual flow rates are equal ($x=y$). The line allows the data to be compared and discussed more clearly. The closer to the line the results are, the less variability between the two sets of results generated. In theory, the data points should be equal and fall along the orange line as they measure the same variable. However, differences in the techniques and methods used to derive them, like channel slope, result in differences between the results generated. The obvious outlier (flow of $95\text{m}^3/\text{s}$) in the figures above was initially attributed to a 75% difference in the estimates of channel slope produced by the semi-automated and manual methods. However, as figure 23 shows, there is no corresponding outlier as would be expected, and it is presumed therefore that this point is instead the result of error.

The three figures show that the manual method produces a lower flow rate than the flow rate estimated by the semi-automated process for all but a small selection of cases. A lower flow rate produced using the manual method means that the stream crossing designed will have less capacity than if it had been designed using the semi-automated method. The lower capacity could potentially lead to damage occurring to the crossing and environment during a 1-in-20-year flood event. However, if the semi-automated method overestimates the flow, the crossing would be over-designed, resulting in an economic loss.

It is noted that the semi-automated process does overestimate the average channel slope, as discussed above. Therefore, the difference in flow rate between the average and equal slope area methods would be less than what is shown in figures 24, 25 and 26. However, the equal area and true average slope measurements still vary significantly in their estimations of channel slope. As such, the equal area and true average slope flow values would follow a similar relationship to that displayed in the figures above, just with a slightly smaller difference in flow rate.

To investigate the channel slopes effect on flow rate, the percentage difference of channel slope and flow values for the same time of concentration equation can be graphed and compared. Figures 27, 28 and 29 follow and allow these comparisons to be undertaken.

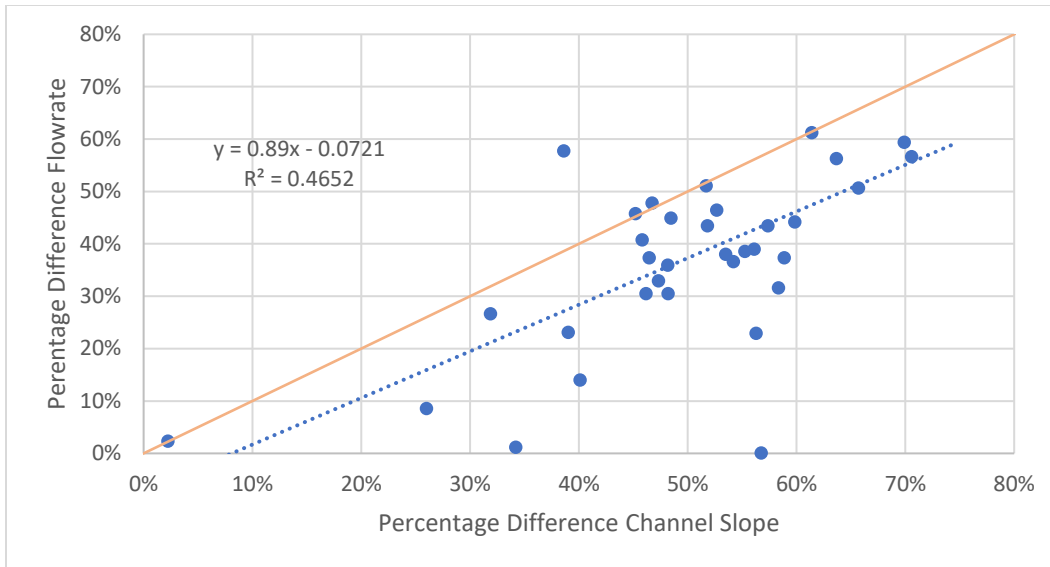


Fig 27. The percentage difference in flow rate and channel slope for the TM61 method utilizing Kirpich's time of concentration equation.

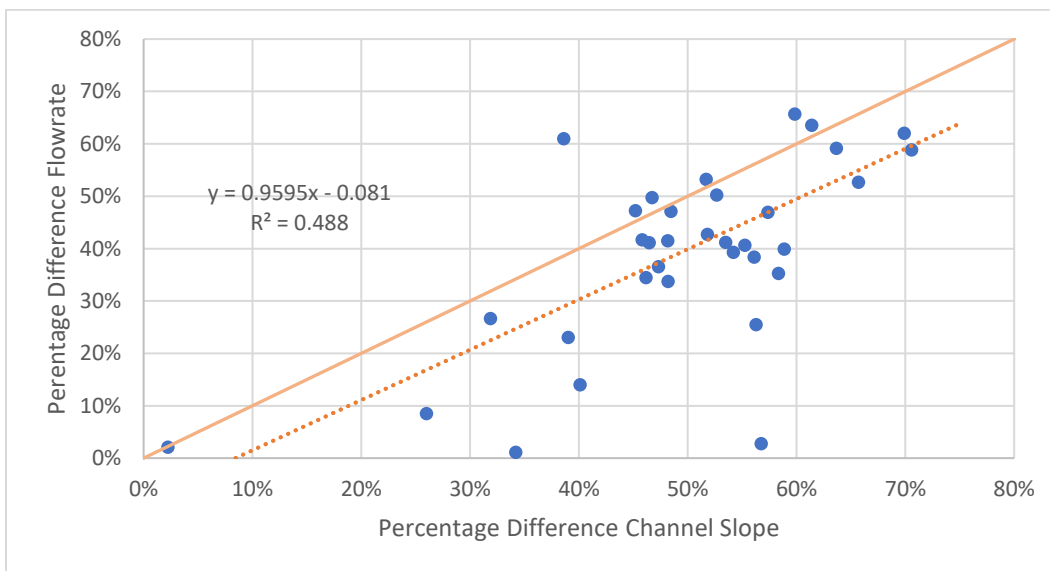


Fig 28. The percentage difference in flow rate and channel slope for the TM61 method utilizing U.S. Soil Services time of concentration equation.

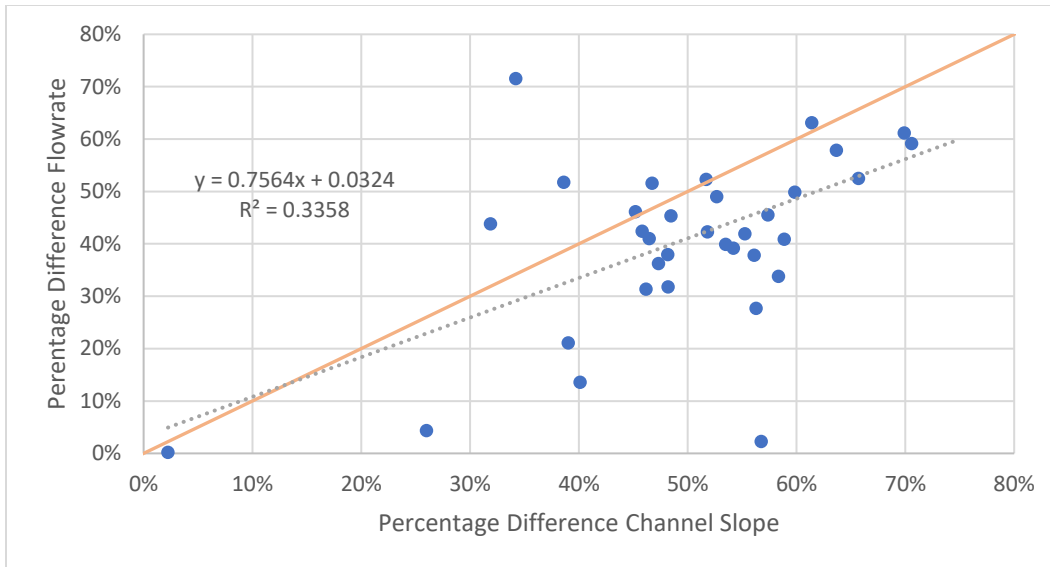


Fig 29. The percentage difference in flow rate and channel slope for TM61 method utilizing William’s time of concentration equation.

The orange line in figures 27, 28 and 29 shows where all the variability in flow rate is explained by the differences between the two channel slopes used (semi-automated and manual). Figures 27, 28 and 29 highlight that the difference in channel slope is larger than the difference reported in the final flow rate (data points below the orange line where $y=x$). Therefore, some of the variability associated with the differences in the average slope is reduced during the TM61 design procedure. However, while there is some reduction, there is still a significant difference between the final design flows calculated. The channel slope is the largest contributing factor to this flow rate difference, highlighting the importance of correctly calculating the channel slope.

5.2 Time of Concentration

A secondary aim of this study was to improve the understanding of time of concentration equations. Three time of concentration equations given by the Ministry of Works and Development (1980) in their TM61 handbook were used to form a comparison. Figure 30 shows how the time of concentration varied across the catchments designed.

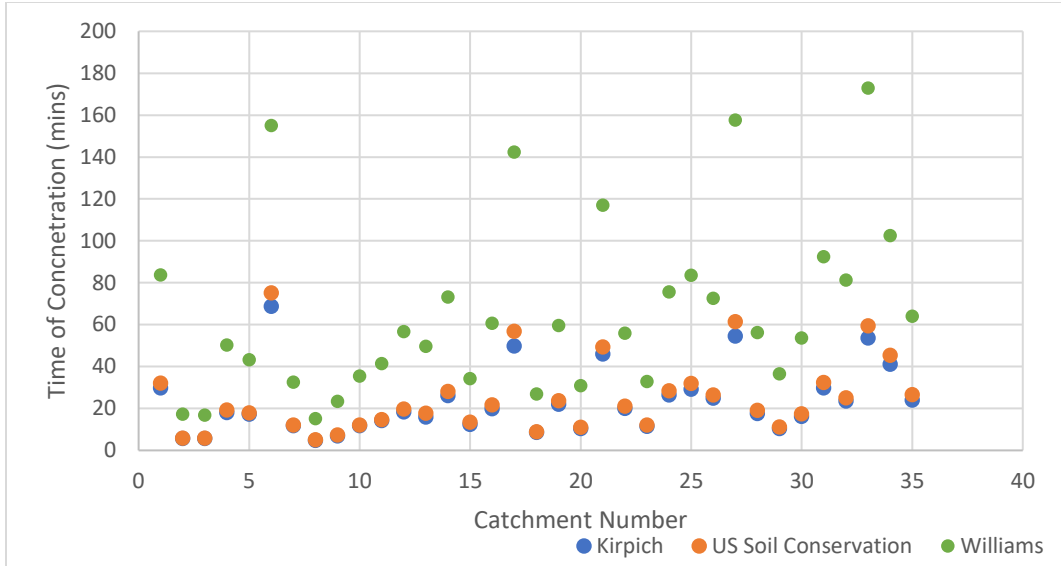


Fig 30. Semi-automated rational time of concentration values.

Only the semi-automated rational set of time of concentration values were explored to ensure results were not repeated. Figure 30 shows that both Kirpich and the U.S. Soil Conservation time of concentration methods produce very similar results with minimal difference between the two. Figure 30 also shows that Williams’s method comparatively always produces a time of concentration value which was the largest. The effect that these trends had on the design flows calculated for the rational and TM61 methods is displayed visually in figures 31 and 32.

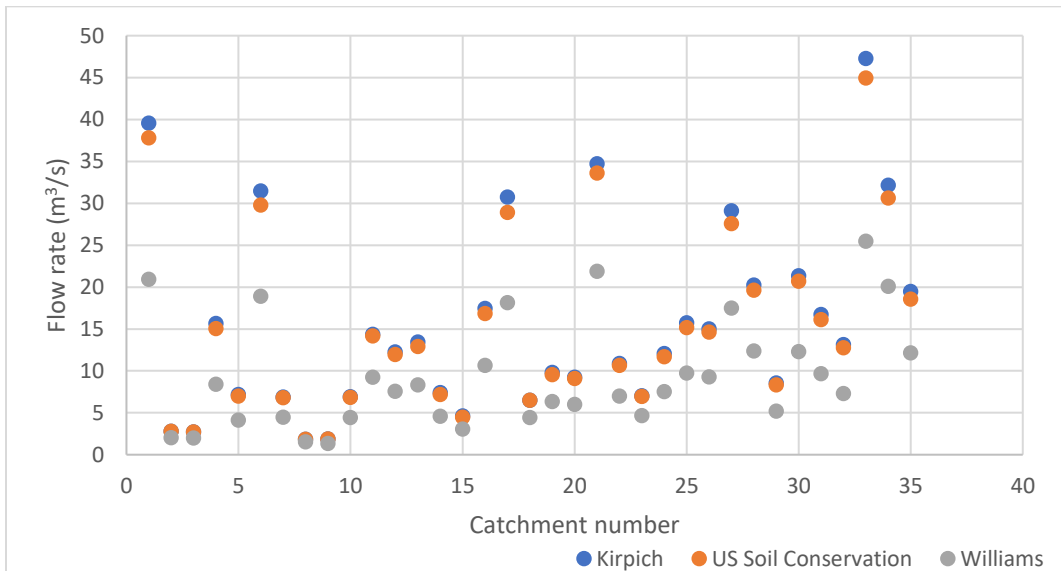


Fig 31. Flow rate from the rational method for each time of concentration equation used.

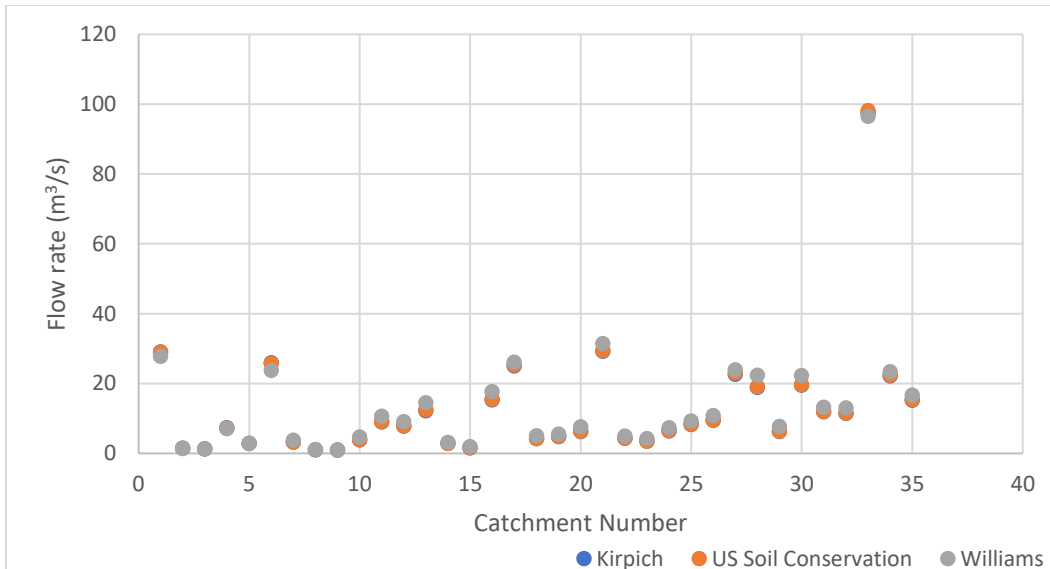


Fig 32. Flow rate from the TM61 method for each time of concentration equation used.

Figures 31 and 32 show the impact that time of concentration plays when undertaking the rational and TM61 design processes. Figure 31 shows that the flow rate the rational method produces is significantly dependent on the time of concentration equation used. Kirpich, followed closely by the U.S. Soil Conservation equation, produces the largest design flow, with Williams equation producing a noticeably lower design flow. The difference in flow rate can be attributed to the influence that time of concentration directly plays on the rational flow estimate. The intensity of the design storm is directly derived from the time of concentration, and for longer times, it is lower. The derived rainfall intensity is then used directly in the flow calculation (one of the three variables multiplied together). Therefore, as shown in figure 30, Williams's time of concentration equation produces the largest time and would subsequently have the lowest rainfall intensity. As a result, William's time of concentration will cause the lowest flow values as explained above and which is replicated in figure 31.

Comparatively, to the rational method, the TM61 design process is relatively not affected by a different time of concentration equation. The lack of effect that time of concentration plays on the TM61 estimate is shown in figure 32, with all three values being relatively comparable. One notable trend in figure 32 is that U.S. Soil Conservation tended to be on the lower side and Williams on the higher side of the flow rates generated. The closeness of the results generated by the TM61 method across the three time of concentration equation helps to give confidence that the design values being produced are reasonable.

5.3 Equation evaluation

The semi-automated method relied on several equations developed to represent nomograms. A selection of these equations were taken from Environment Waikato (2006), and two were created using a polynomial approximation procedure within excel. The equations were evaluated separately during the design procedure as the values produced by the manual and semi-automated methods were different, so a direct comparison could not be made between the two. The equations were only evaluated using design values produced using Kirpich's time of concentration method. Table 7 follows and contains a selection of the equations evaluated using linear regression alongside their respective r^2 values. Table 7 also includes

the average percentage difference between the manual and semi-automated methods and the range the equations were evaluated across.

Table 7. Equation evaluation.

Parameter Name	Equation Number & Source	r ²	Avg. Percent Difference (%)	Range Evaluated
Slope Coefficient (W _s)	10 - Literature	0.9964	0.95	36.5 – 80.5
Discharge Coefficient (C)	11 - Literature	0.9992	1.9	526 – 2166
Standard rainfall depth (R _{sd})	12a - Literature	0.9988	1.5	35 - 80
Shape Factor (S)	13 – Polynomial Approx.	0.9907	1.3	0.68 – 1.26

Table 7 highlights that the r² values achieved indicate that the linear trendline fitted all four sets of data well. The low average percentage differences between the values derived by the charts and those derived by equations help highlight that the equations represent the charts well. The discharge coefficient (C) had the largest percentage difference, 1.9%, between its chart and equation based values. However, it is noted that the discharge coefficient is directly derived using the slope coefficient, and as a result, the percentage difference is cumulative. Not all of the equations listed in this report that represent nomograms were evaluated. The standard rainfall depth is calculated using two equations dependent on the time of concentration. One equation is used for a time of concentrations less than 120 minutes, and another is used for a time of concentration greater than 120 minutes. Due to the size of the catchments evaluated, the equation which coincides with a time of concentration exceeding 120minutes, equation 12b, was not evaluated.

The impact the equations had on the design flow rates estimated was also investigated. This investigation was completed by comparing the equation and chart-based flow estimates, as shown in figure 33.

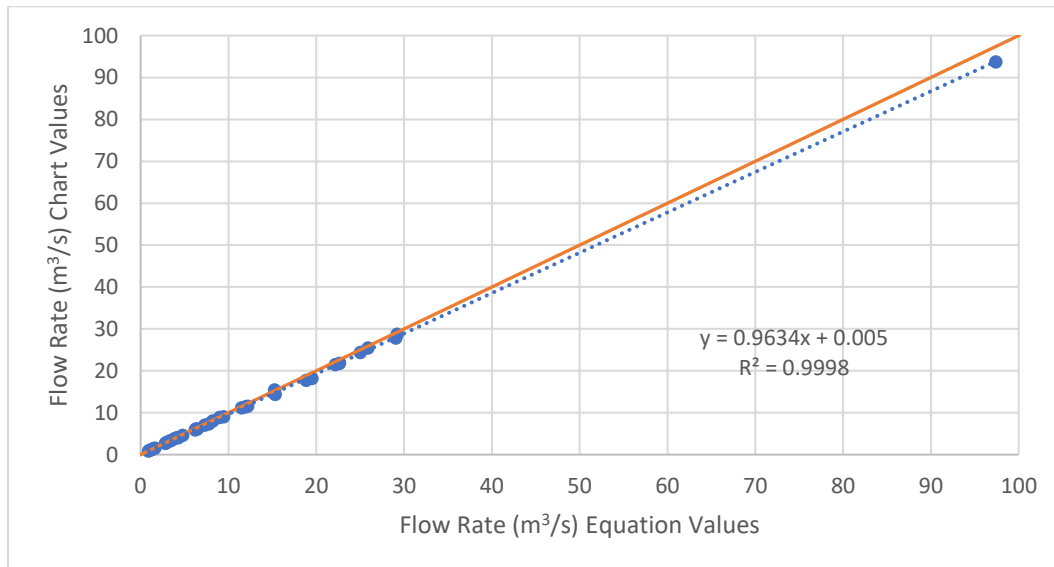


Fig 33. Comparison between the flow rate values derived using both equations and charts.

Figure 33 highlights that the flow rates calculated using the equations are close to those computed using charts. However, it is noted that in figure 33, the trendline and values tend to be on the lower side of the orange line, indicating that the values produced using the equations are higher than those produced using

the charts. On average the flow rate calculated using the equations was 3.6% larger than one produced using the charts. While the equations overestimating the design flow is not ideal, the overestimate is not too large that it negatively inhibits the design of the crossing. More importantly, the flow values produced by the equations are not less than those derived from the charts, as it is thought that an underestimate of the design flow would likely be more detrimental than a slight overestimate.

The final equation to be checked in terms of its accuracy was for culvert sizing, and it was derived using a polynomial approximation. Figure 34 follows and contains the comparison between the equation and chart values for culvert sizing.

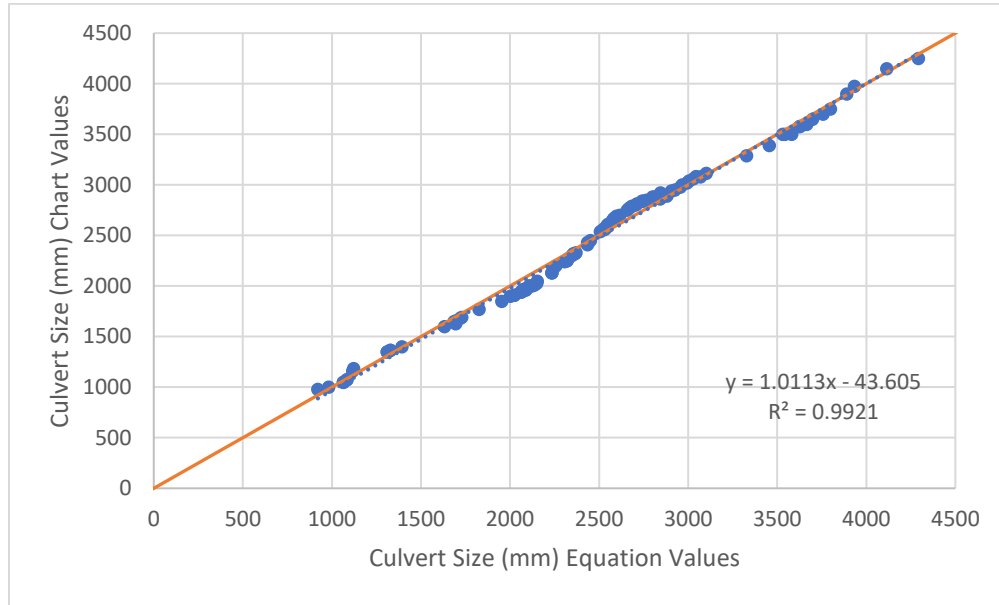


Figure 34. Comparison between the culvert sizing values derived using either equation or chart.

Figure 34 highlights that a large proportion of the culvert chart was evaluated regarding its suitability at being represented by equation 13. It was found that equation 13 (as given) tended to give culvert diameters significantly different from those obtained using a chart. The significant differences were eliminated by increasing the equation of the trendline given in excel to 8 decimal places to ensure that the equation was fully representative of the polynomial trendline it was portraying. The polynomial nature of the approximation equation is evident in figure 34, with a similar curve appearing in figure 18. The absolute average and average percentage differences between the equation and chart based values was 61mm and 2.7% respectively. The variations in culvert diameter ranged from a maximum underestimate of 106mm to a maximum overestimate of 129mm. While these two values were the maximum differences obtained, they help highlight the scale of the variability associated with using the equation presented to calculate the culvert diameter.

5.4 Time Evaluation

One of the semi-automated process's key objectives was to help save designers time and be a practical alternative to the manual design process. Therefore, the semi-automated processes needed to be at a minimum as good as doing it manually, if not better than it. For example, if the semi-automated process took considerably more time to complete the design than its manual counterpart, the actual effectiveness

and practicality of the process would be negligible. To evaluate the practicality of the semi-automated method, the design time of each catchment was recorded.

The design process was split into timing segments to allow a more in-depth evaluation to be undertaken. For example, the rational method was divided into three parts. The first part included deriving the catchment characteristics (area, longest flow path). The second part was the runoff coefficient derivation, and the third was the final design calculations. Similarly, the TM61 method was also split into three parts. However, the first part was the same as the rational methods and didn't need to be repeated. The second and third steps were the cover coefficient selection (W_{ic}) and final calculations, respectively. The average design times across the 35 catchments for both the semi-automated and manual process follows in table 8.

Table 8. The average design times for both the semi-automated and manual methods.

Semi-automated - time in minutes (decimal)							
Rational				TM61			
Time Part 1	Time Part 2	Time Part 3	Total Time	Time Part 2	Time Part 3	Total Time	Total Design Time
5.9	3.3	3.6	12.8	2.2	4.4	6.6	19.3
Manual - time in minutes (decimal)							
Time Part 1	Time Part 2	Time Part 3	Time Total	Time Part 2	Time Part 3	Time Total	Total Design Time
7.9	6.1	3.0	16.9	0.8	9.8	10.6	27.5
Percentage difference							
-35%	-82%	18%	-32%	64%	-120%	-60%	-43%

Table 8 shows that the semi-automated process has an average time saving of 43% or around 8.2 minutes. The time saving of the semi-automated process helps to demonstrate that it achieves both the goal of saving designers time and the required practicality. The average saving of 8.2 minutes does seem on the smaller side. However, an average time saving of 8.2 minutes across 35 catchments is quite significant and equates to 4.8 hours' worth of time saved.

Table 8 also highlights the parts of the design process which have the largest differences in design time. The runoff coefficient selection has a significant time difference of 82%. The difference here can be attributed to the time taken to work out the different contributing land covers across the catchment and measuring the area these take up manually. Part 2 of the TM61 process showed that undertaking this step manually resulted in a significant time-saving. The time saving resulted from the information gathered in part 2 of the rational method manual process being able to be reused. The pre-gathered information meant that the proportion of land covers could be easily calculated, and the measurement process did not need to be redone. The most significant time saving of the semi-automated process was with step 3 of the TM61 process. On average, the semi-automated process was 43% quicker than that of its manual counterpart. The time saving can be attributed to implementing the calculations as a replacement for undertaking the same design process using charts (nomograms).

In an attempt to further explore how the total catchment design time is influenced, a comparison will be made between design time and catchment size. Figure 35 follows and shows how the total catchment design time varies in relation to catchment size.

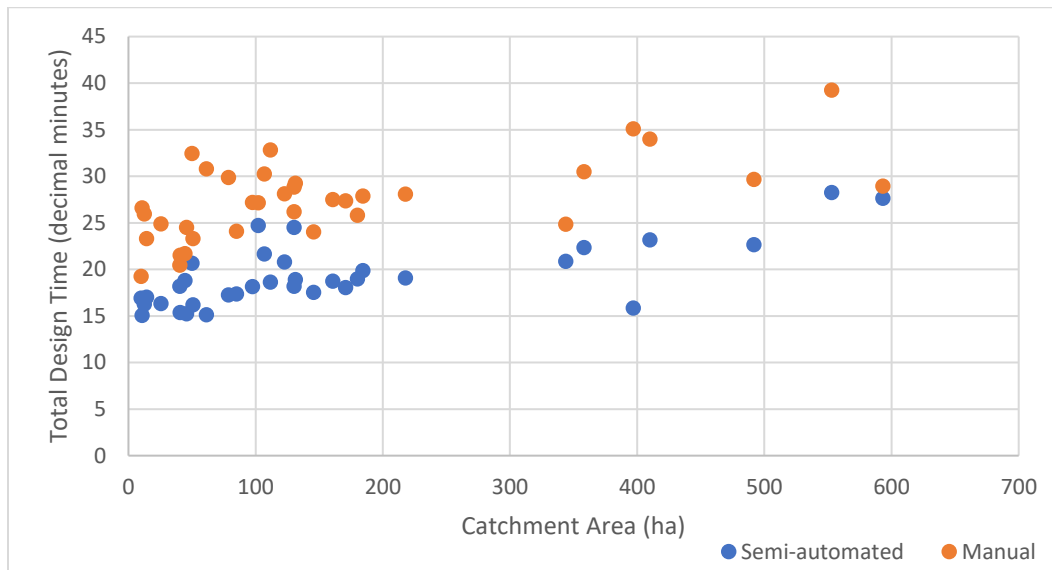


Fig 35. Catchment area and total design time.

Figure 35 shows that as catchment size increases, both semi-automated and manual total design times increase also. The increasing trend in both catchment area and design time is expected. However, it was anticipated that the differences between the semi-automated and manual design times would be more significant at larger catchment sizes. Two outliers (around 130ha and 100ha) from the semi-automated process are also observed in figure 35 at smaller catchment sizes. Both the two outlier's and the minimal difference in design time as catchment size increased are likely due to the first step of the model for deriving the catchment characteristics. This step required more processing time as the catchment size increased, with the script for deriving the longest flow path being the key contributor to this longer processing time. In conjunction with this increase in processing time, the step needed to be rerun to increase the snapping distance of the tool on occasion to ensure an appropriate catchment was built. Figure 36 plots the design time of the catchment characteristics (part 1) against catchment area.

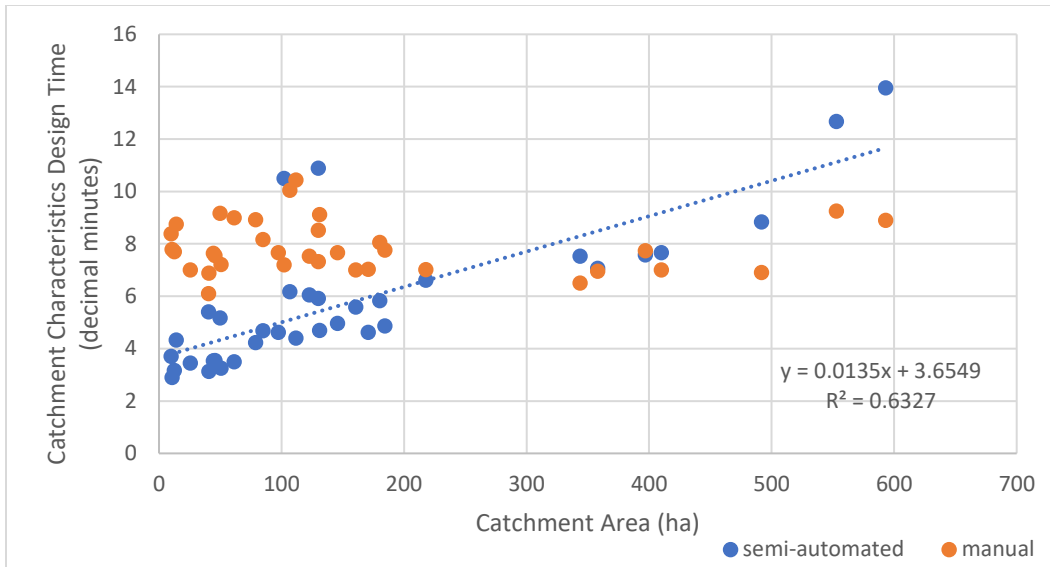


Fig 36. Catchment area and catchment characteristics design time (part 1).

Figure 36 adeptly highlights the two catchments discussed above that are significant outliers (catchments with sizes of 130ha and 100ha). These two catchments were outliers because they needed to be rerun at least four times each before an appropriate catchment was built. Other catchments also needed to be rerun over the course of the study. However, these were the two most notable cases and the effect the reruns had on the design times is worth highlighting.

5.5 Runoff Coefficient

Another secondary aim of this study was to improve the design procedure around the selection of the runoff coefficient. The manual and semi-automated runoff coefficient calculation processes were quite similar and revolved around calculating a weighted runoff coefficient. It was found during the design process that both these methods were achievable, did not rely significantly on user experience or bias and were a more rigorous and structured design process than the current methods used. While these methods generally performed very well, an issue was identified with the semi-automated process relating to the land cover database (LCDB) layer. While providing a generally good representation of the land covers, the layer would, on occasion, oversimplify the land cover, and smaller patches would not be defined. An example of the land classes being simplified is shown in figure 37.



Fig 37. Land cover simplification (aggregation).

In figure 37, the LCDB classes are denoted with an orange boundary, and the catchment boundary is shown in red. The LCDB layer overlaying the aerial imagery confirms that the layer provides a good representation of the land classes' boundaries within a catchment. However, figure 37 also highlights the issue of smaller areas of a land cover being aggregated as part of a different land class. An example of this issue is outlined in blue in figure 37, which shows a patch of scrub/native being classified as part of a commercial forest. These areas can be corrected during the design procedure to remove this misclassification. However, this correction process would result in the semi-automated process producing varied results from person to person (not everyone will distinguish the boundary's the same). While this oversimplification is not ideal, its effect is not a significant cause of concern within the commercial forestry boundary class. The areas are relatively small, and a slightly higher C value is produced, which is more conservative.

It would appear that the manual design process would allow for a slightly more representative delineation of the land covers within the catchment compared to the semi-automated process. However, the manual process relies on the user conducting it to take the time to delineate all the land covers accurately. The scale that the user identifies and delineates the different land classes at also provides another potential error source. An example of the error delineation scale can produce follows in figure 38.



Fig 38. Mapped land class compared at two different scales (1:10000 left and 1:1000 right).

Figure 38 shows an area outline in blue that has been delineated at a scale of 1:10000 (lefthand image) and another image of the same area mapped at 1:1000 scale (righthand image). The image on the left shows that the area outlined in blue gives a decent representation of the border between the two classes. However, the image on the right focused on the top end of the drawn polygon shows that the delineated area overestimates the land class with the actual boundary line highlighted in red. The horizontal difference between the true and drawn boundary is around 8-10 metres which is significant. Figure 38 helps to highlight this error and shows how a boundary that looks relatively well-drawn can still be incorrect.

Regardless of the problems listed and described above, both the semi-automated and manual procedures performed the runoff coefficient design process well. A comparison between the runoff coefficients calculated for the manual and semi-automated processes follows in figure 39.

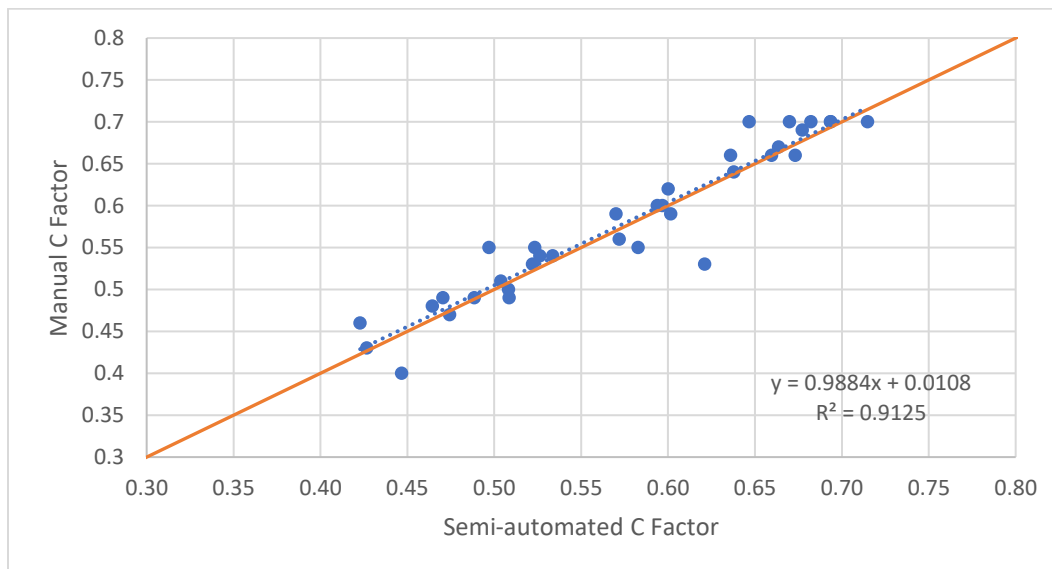


Fig 39. Comparison between the C factors generated using the semi-automated and manual methods.

Figure 39 shows a general agreement of the values and highlights that one could use either the semi-automated or manual method to get a reasonable representation of the runoff coefficient, which is reflected by the average percentage difference between the two being 3.4%. The general consensus in the values instils confidence that the processes used are viable methods for determining a runoff coefficient value. A noticeable trend of figure 39 is that the manual method gives slightly higher C values which is indicated by the trendline sitting above the orange line, which indicates where the variables would be equal ($x=y$). The data grouping around the trendline is quite tight, with an r^2 value of 0.9125, confirming this. Table 9 follows and contains a brief analysis of the benefits and disadvantages associated with both methods.

Table 9. Benefits and disadvantages of the manual and semi-automated design procedure for the runoff coefficient.

Semi-automated		Manual	
Benefits	Disadvantages	Benefits	Disadvantages
Requires minimal interaction.	May not represent the smaller patches of different land covers within the catchment.	Can delineate smaller areas to get a better representation	Can oversimplify some areas in relation to the soil and slope representation across the catchment.
Repeatable results will be generated even when different people use the model (as long as the same proportions of harvested areas are used).	The user does not have as much interaction (not as immersive) with the data, so the result produced cant have a simple reality check done (only real problem for new designers).	A simple process that doesn't require experience or judgment to estimate an appropriate value (compared against the current design procedure).	Different people will get different results even for the same catchments.

6. Discussion

6.1 Channel Slope

The channel slope was identified as the factor which differed the most between the semi-automated and manual processes. As discussed above, another method referred to in this study as 'average points' was used to evaluate the semi-automated and manual channel slope measurements. It was found that the semi-automated method overestimated the average channel slope on average by 21%. Therefore, the final flow values produced using the semi-automated process will also be an overestimate of the actual 1-in-20 year flow values.

As described in the result section (5.1.3), the average points method is an overcomplicated way of deriving the channel slope. The measure of channel slope the average points method derives is equivalent to a channel slope calculated using the minimum and maximum elevation points along the stream channel. With the knowledge that the endpoints of the flow path can be used to derive a more representative average slope than the semi-automated process, a simple alteration of the code used in the semi-automated process is all that is required to employ this method. Calculating the average slope using the channel's endpoints (minimum and maximum elevations), the average percentage difference between the semi-automated and manual processes would be less, and the semi-automated process would no longer be overestimating the average channel slope.

While the average points and equal area method are not directly comparable, the average difference of 41% between the two measures of channel slope is significant. It is not known which of the two measures best represents the actual channel slope. As such, a definitive answer cannot be given as to whether one is overestimating or underestimating their respective measures of the channel slope. However, as stated above, the average difference of 41% between the two methods is quite significant, and the impact this

has on the flow values generated is substantial. To further evaluate the average points and equal area methods, a brief search through literature was conducted.

Vianello, Cavalli and Tarolli (2009) compared different methods of computing channel slope using varying resolutions of 1m, 2m, and 5m derived from a LiDAR digital terrain model. The methods used by Vianello, Cavalli and Tarolli (2009) were not identical to the average points method used above. However, the longitudinal profile method they employed does have some similarities. The longitudinal profile method uses distinct features within the channel as the increments at which it calculates stream slope across instead of set increments of length like the average points method. The method was found to slightly underestimate the slope of the stream compared to the infield measurements but performed the best out of the methods evaluated.

Neeson et al. (2008) examined the accuracy of GIS-derived stream slopes for a set of stream reaches in Idaho and Ohio. The DEM used in this study had a grid cell size of 10m, and it is thought that the coarseness of the data used will have likely impacted their results. The techniques used were similar to the average points method except that the incremented distance the slope was calculated over was split into reaches. A reach is a section of a river or stream for which the same hydrological conditions exist. The reaches were measured in the field for their slope, which was then compared to that produced using the GIS elevation data. The length of the reaches evaluated varied but were typically more than 100m. Neeson et al. (2008) found that for the Ohio data set, GIS slopes were larger than the field slopes, and the opposite was true for Idaho, meaning a definitive trend was not established from the data.

While the two papers discussed above do not evaluate the average slope method directly, each helped highlight areas of difference. Both Neeson et al. (2008) and Vianello, Cavalli and Tarolli (2009) field surveys split the channel into uniform segments and evaluated these segments in terms of their slope. Comparatively, the average slope method takes the average of the entire stream channel regardless of the stream's properties along the channel. Vianello, Cavalli, and Tarolli (2009) also highlighted that a cell by cell local slope along the stream length could be higher than a corresponding field slope measured along the reach due to the presence of steps, cascades, and rock outcrops. Therefore, it is thought that the average slope measurement derived in this study could potentially overestimate the channel slope compared to a field measurement.

A search for literature evaluating the equal area method produced limited results. Ministry of Works and Development (1980) provides only a brief explanation on how to use the method with no indication of where it was developed for and why. Ladson (2017) highlights that the method was likely developed as a more representative alternative than the average slope derived from the start and end points of the stream. Ladson (2017) also states that the method would have been easy to calculate pre-computer times, and the method seems to have been largely forgotten. The lack of research evaluating the equal area method and even describing its origins highlights both a potential gap in research and leads to questions about its suitability for designing waterway crossings in New Zealand.

The channel slope evaluated in this study was derived from the longest flow path. In this study, the longest flow path was taken from the desired catchment outlet to the furthest draining cell (often on the catchment boundary). According to the Ministry of Works and Development (1980), the W_s factor requires the "horizontal length and slope of the main channel extended up to the catchment boundary". Therefore, taking the longest flow path to the edge of the catchment aligns with the TM61 design process. It is also

anticipated that the definitions given by the Ministry of Works and Development (1980) are carefully worded as the nomograms they present would have been calibrated using these definitions.

One area that the longest flow path was thought to have affected was the time of concentration equations. The longest flow path used in this study incorporates portions of both overland and channel flow. The effect of the inclusion of both overland and channel flow is that for Kirpich's time of concentration equation, only the channel flow proportion should have the equation applied to it (Ravazzani et al., 2019). The Ministry of Works and Development (1980) contested this statement by specifying for Kirpich's equation that the flow length is "from the furthest point on the catchment to the outlet". Due to the Ministry of Works and Development (1980) being stated as one of three key design documents under the NES-PF, its definition of the flow length is taken to be the most appropriate.

Extending the longest flow path to the edge of the catchment results in a larger average channel slope than if only the portion of the stream that exhibits channel flow properties is accounted for. The difference between the equal area and average channel slope measurements is also anticipated to decrease if only the channel flow proportion of the stream is measured. The decrease is expected due to the alteration of the stream profile (removing the top steep proportion). However, how much the decrease in the difference would be is not known. It is also questioned whether the equal area channel slope derived for the flow path to the edge of the catchment is similar / representative of the average channel slope derived for the channel flow proportion of the stream. However, this thought was not investigated further as it was outside the scope of this study, but it highlights a potential area for further research.

If the longest flow path used in this study was found to be an area that needed to be changed, an alternative method could easily be developed in ArcGIS. One alternative approach that was explored included having a set number of drainage cells before the flow path begins in order to reduce the effects of the overland flow proportion on the results. This method was briefly investigated to ensure that it would work, but it was not explored in detail. It was also identified that perhaps the equal area method could potentially be a more representative measure of the stream slope, but further research would need to be conducted on this topic to make this assertion with confidence. If the equal area method was determined as the most representative measure, the equal area process could be undertaken using an equation-based methodology. Gericke and Du Plessis (2012) give a set of equations that can be added to a methodology like the average points one described above, allowing the equal area process to be determined automatically without the human graphical element.

6.2 Time of Concentration

Three time of concentration equations were explored in this study using both the rational and TM61 processes. The TM61 process showed that the time of concentration equation used was largely independent of the discharge result generated, with the flow values produced from all three equations being roughly equal. It should be noted that the flow values generated for each of the three time of concentration equations were not identical but they were close to one another. The closeness of the design values produced gives confidence in the values produced and highlights that for the TM61 process, either of the three equations is appropriate for flow estimation. However, by using all three equations during the design process provides a good reality check and helps to eliminate any significant human error made in the process.

Comparatively to the TM61 process, the rational process was severely affected by the different time of concentrations calculated by each of the three equations. The significant effect the rational method experienced was due to the direct implication the time of concentration had on the design flow calculated. To ensure a conservative flow estimation is made using the rational method, either Kirpichs or the U.S. Soil conservation equation should be used to calculate the time of concentration.

6.3 Equations

The equations used to help facilitate the semi-automated process produced results primarily agreeable to those produced using the charts said equations were derived from. Two types of equations were used; equations provided by literature and derived using a polynomial approximation. The equations taken from the literature performed well, with the typical average percentage difference between the equations and the chart-based values being less than 2%. Not all equations listed in this study were evaluated, with the R_{sd} equation for a time of concentrations exceeding 120minutes not being assessed due to the data sample used.

The polynomial equation also approximated the shape factor well, with the average difference between values derived from the equation and chart values being 1.3%. It should be noted that a relatively small proportion of the shape factor chart was evaluated: between 0.7 and 1.3. Therefore, for catchments with differing geometry (size and shape) to those assessed in this study, the actual performance of this polynomial approximation is not known. However, based on how it performed for the range evaluated in this study, it is thought that it will likely also perform well across the entire range of values. It is also worth mentioning that the polynomial approximations provide a good representation across the range of data points they are created from. Outside this range, the approximations go haywire due to the nature of the polynomial curve, as shown in figure 40. Therefore, bounds need to be specified on equations derived using this method and are typically taken as the two endpoints of the data.

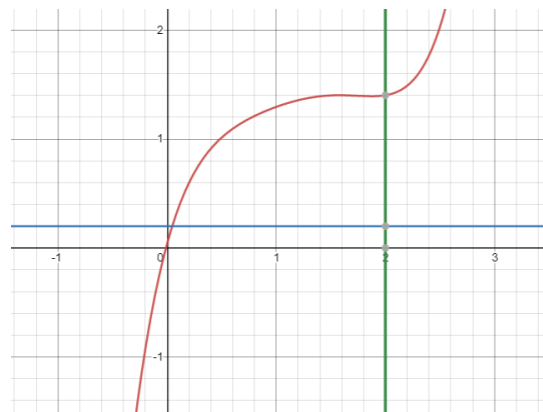


Fig 40. Shape factor equation behaviour outside data range.

Figure 40 was plotted using the desmos graphing calculator and shows the behaviour of the approximation equation outside the range given on the chart. The blue and red lines highlight the bounds of $y = 0.2$ and $x = 2$, which provide the range that the approximation is valid across. Figure 40 helps to highlight the issues discussed above and the importance of staying within the bounds of a polynomial approximation.

The combination of the equations from literate and the polynomial shape factor equation led to flow values which, on average, were 3.5% larger than those derived purely by charts. The flow overestimates made by the equations is not too drastic and allows a user to use them confidently, knowing that they will not give results significantly different to those calculated using charts. Once again, it should be highlighted that these equations were not evaluated across the entire range they represent. However, over the range they were assessed, they performed well and could be used instead of charts with confidence.

A benefit observed while comparing the results generated by the charts and equations was that the equations generate one unique result (given they are used correctly). Comparatively, designers using the charts will inherently get different results due to human error, poor technique, and even the thickness of their pencils led. Therefore, it is anticipated that using the equations will lead to a more consistent design independent of the user.

The second equation derived using a polynomial approximation was used for culvert sizing. The culvert sizing equation was evaluated in-depth, with 105 comparisons made between it and values derived from charts. The assessed values were also well spread out over the charts entire range. It was determined that the equation caused a significant amount of variability, even after increasing the equation to 8 decimal places, in the results achieved using it and those derived using charts. The range of variability found during the evaluation was a maximum underestimate of 106mm to a maximum overestimate of 129mm. Therefore, it is felt that for deriving the culvert sizing, the equation developed is not as practical and accurate, and as a result, it is recommended that the chart is used instead.

6.4 Time Evaluation

Timing the design process was used to evaluate the semi-automated processes viability and practicality. It was found that, on average, the semi-automated design had an average time saving of 43% or around 8.2minutes. One key issue identified that could reduce the effectiveness of the semi-automated methods was the issue of an increased processing time as catchment sized increased. For the catchment sizes evaluated in this study, which primarily represented those typically designed for in New Zealand's forest industry (400ha or less (Costley, 2018)), processing time did not hinder the design. It should also be noted that the laptop used to complete the study is seven years old, and as such, it is anticipated that a more modern machine would have a quicker processing time. The semi-automated process's key areas that produced a significant time saving included the derivation of the runoff coefficient and the final design using equations for the TM61 process.

6.5 Runoff Coefficient

The runoff coefficient values produced using the semi-automated and manual processes were largely agreeable, meaning that either process could have been used to produce a viable value. Two notable sources of error were also identified during the evaluation, including the land cover database (LCDB) layer oversimplifying some areas of land cover and the effect of delineating land covers at different scales.

One potential shortcoming in the analysis undertaken of the runoff coefficient is the different 'accuracies' of the spatial data used in it. The LiDAR-derived digital elevation model (DEM) is highly accurate with a spatial resolution of 1m². Comparatively, both the FSL soil drainage and LCDB layers metadata state they have typical scales of 1:50000. The accuracy of the LCDB layer was investigated visually during the study by comparing it to aerial imagery. Comparing the LCDB layer with the aerial imagery allowed the effectiveness at which it mapped the land covers to be explored. It was found that while the LCDB

generally performed well, it did oversimplify some areas. The oversimplification of these areas was the most significant error found in the semi-automated process for determining the runoff coefficient. The scale the LCDB is mapped at, 1:50000, is thought to cause the simplification error as the areas could have been potentially too small to delineate effectively by the model which created the layer.

Unlike the LCDB layer, a visual comparison could not be made to evaluate the FSL soil drainage layer. Therefore, the accuracy of the soil drainage layer across smaller areas, like some of the catchments assessed, cannot be guaranteed without an infield survey. However, the layer provides a reasonable basis for one to work from, and the inclusion of the effects of soil only helps increase the processes reliability. While searching for soil spatial data that would allow the design process to be undertaken, a new soil layer called S-map developed by Manaaki Whenua (Land care Research) was identified. While having the same scale as the FSL soil drainage layer, the S-map provides a more comprehensive and up to date data source. The S-map layer does not have full coverage of New Zealand yet, so it could not be used in the analysis. However, the development of new spatial data like S-map is a notable trend where more reliable, detailed, relevant (timely), and accurate data is becoming more widely accessible and available. This trend highlights that processes like the one undertaken in this study will become increasingly achievable and be able to be completed with more confidence.

The manual process undertaken did oversimplify both the soil and slope contribution to the runoff coefficient. However, there was not much difference between semi-automated and manual runoff values generated, as discussed above. It is thought that the oversimplification of the soil contribution did not affect the runoff coefficient severely due to the coarse scale of the data layer used. If the layer were to increase in detail, the method used to approximate the soil's contribution manually would likely increase the oversimplification. Subsequently, the difference between the runoff coefficient produced using this technique and the semi-automated process would increase in magnitude.

One of the most significant benefits of the semi-automated process compared to that of the manual process was similar to those highlighted above regarding the use of equations. The results generated by the semi-automated process were repeatable, with users being able to generate the same result for a catchment (as long as the same land cover proportions are used, harvested v not). The semi-automated process also removed human error and bias largely from the process.

7. Conclusion

The purpose of the study undertaken was to develop and evaluate a semi-automated design procedure created within ArcGIS for culvert design. In addition, the semi-automated process also needed to be practically feasible and produce results that were accurate and repeatable. Thirty-five catchments were designed for using both the semi-automated and manual processes to allow a comparison and evaluation to be formed between the two methodologies. A key focus was also placed on the runoff coefficient and time of concentration equations to investigate the impacts these have on culvert design.

The study showed that the semi-automated process developed was practical by both saving designer's time and producing repeatable results. The accuracy of the results produced was questioned due to the variability associated with the average channel slope measurements. However, the semi-automated process could be easily altered to correctly calculate the average channel slope, reducing some of the variability. With the correction made to the average slope, the semi-automated processes results could

be deemed 'accurate'. However, it is noted that the variability between the equal area and average slope measurements of channel slope even after the alteration is applied was significant.

Upon consulting some literature, it was anticipated that perhaps the average slope measurement derived in this study could overestimate the channel slope compared to an infield measurement. But a lack of information around highlighting the equal area methods suitability meant that a definitive answer could not be established as to which method is the most suitable for determining the average channel slope. Subsequently, it is felt that channel slope is an area where further research could be conducted due to the severe implications it has on the design flows calculated.

Several equations were required for the semi-automated process to be completed. It was found that the equations from literature and the polynomial approximation of the shape factor chart all performed well. However, the polynomial approximation of the culvert chart did not perform as well, and it is recommended a nomogram remains in use for culvert sizing.

The processes used to calculate the runoff and W_{IC} coefficients for semi-automated and manual methods worked well. Both the manual and semi-automated processes produced agreeable results. The semi-automated process was, on average, 80% quicker than the manual method and removed a large amount of potential human error from the process. The design method used for both the runoff and W_{IC} coefficients was slightly different to the methods currently used in the forest industry. However, it was felt that the new methodology allowed for a better design by being more structured and by reducing the reliance on user 'experience' in determining an appropriate value.

One of the key highlights of the semi-automated process was reducing human interaction and errors produced during the design process. Meaning that if two people were to run the semi-automated process, they would produce results that, barring user error, would be identical. Overall, the semi-automated process developed worked well. It is thought that the process does need further work, with two notable areas being the average channel slope and longest flow path. However, this study highlighted that the process is both physically feasible and practical, underlining further potential to expand on and employ the work completed in this study.

References

- Allum, J., Luff, N., Le Lievre, A., Riedinger, L., Walsh, J., McCormack, D., & Chen, X. (2020). *Recommendations for culvert sizing in the New Zealand forest Road Engineering Manual*.
- Azizian, A. (2019). Comparison of salt experiments and empirical time of concentration equations. *Proceedings of the Institution of Civil Engineers – Water Management*(172(3)), 109–122. doi:<https://doi.org/10.1680/jwama.17.00048>
- Blagojević, B., Kovačević, S., Ned, B., Lukovac, N., & Mujčić, M. (2018). GIS Based Flood Flow Assessment in Small Catchments for Flood Mapping in Bosnia and Herzegovina. *Ovidius University Annals of Constanta-Series Civil Engineering*, 20(1), 111-118.
- Bondelid, T., McCuen, R., & Jackson, T. (1982). Sensitivity of SCS Models to Curve Number Variation 1. *JAWRA Journal of the American Water Resources Association*, 18(1), 111-116. doi: <https://doi.org/10.1111/j.1752-1688.1982.tb04536.x>
- Brown, K., & Visser, R. (2017). Erosion sources and sediment pathways to streams associated with forest harvesting activities in New Zealand. Retrieved from <https://ir.canterbury.ac.nz/handle/10092/15043>
- Christchurch City Council. (2020). *Waterways Wetlands and Drainage Guide: Part B - Chapter 21*. Retrieved from <https://www.ccc.govt.nz/assets/Documents/Environment/Water/waterways-guide/21.RainfallAndRunoff.pdf>
- Costley, B. (2018). *Culvert Design for New Zealand Forestry*. Retrieved from <https://forestengineering.org/wp-content/uploads/2020/11/2018-Ben-Costley-Final-Report.pdf>
- Department of Building and Housing. (2020). *Compliance Document for New Zealand Building Code: Clause E1 Surface Water*. Retrieved from <https://www.building.govt.nz/building-code-compliance/e-moisture/e1-surface-water/>
- Dooge, J. C. (1974). The development of Hydrological Concepts In Britian and Ireland Between 1674 and 1874. *Hydrological Sciences Journal*, 19:3, 279-302. doi: <https://doi.org/10.1080/02626667409493917>
- Environment Waikato. (2006). *Environment Waikato Best Practice Guidelines for Waterway Crossings*. Retrieved from <https://www.doc.govt.nz/globalassets/documents/conservation/native-animals/fish/fish-passage/waterway-crossings.pdf>
- Environmental Hazards Group. (2012). *Hydrological and Hydraulic Guidelines*. Retrieved from Bay of Plenty Regional Council: <https://www.boprc.govt.nz/media/373948/hydrological-and-hydraulic-guidelines.pdf>
- Fang, X., Cleveland, T., Garcia, C., Thompson, D., & Malla, R. (2005). *Literture Review on Timing Parameters for Hydrographs*. Department of Civil Engineering, Lamar University, Beaumont, 83. Retrieved from https://www.depts.ttu.edu/techmrtweb/reports/complete_reports/4696_complete.pdf

- Fang, X., Thompson, D., Cleveland, T., Pradhan, P., & Malla, R. (2008). Time of Concentration Estimated Using Watershed Parameters Determined by Automated and Manual Methods. *Journal of Irrigation and Drainage Engineering*(134(2)), 202-211.
- Gericke, O., & Du Plessis, J. (2012). Catchment parameter analysis in flood hydrology using GIS applications. *Journal of the South African Institution of Civil Engineering= Joernaal van die Suid-Afrikaanse Instituut van Siviele Ingenieurswese*, 54(2), 15-26.
- Gericke, O., & Smithers, J. (2014). Review of methods used to estimate catchment response time for the purpose of peak discharge estimation. *Hydrological Sciences Journal*(59(11)), 1935-1971. doi:<https://doi.org/10.1080/02626667.2013.866712>
- Greer, A. D., Wilbanks, Z. B., Clifton, L. D., & Wilson, B. (2018). GIS-Enabled Culvert Design: A Case Study in Tuscaloosa, Alabama. *Advances in Civil Engineering*. doi:<https://doi.org/10.1155/2018/4648134>
- Griffiths, G., & McKerchar, A. (2008). Dependence of flood peak magnitude on catchment area. *Journal of Hydrology (NZ)*(47 (2)), 123-131. Retrieved from http://hydrologynz.co.nz/downloads/20110419-045616-JOHNZ_2008_v47_2_Griffiths.pdf
- Griffiths, G., & McKerchar, A. (2012). Estimation of mean annual flood in New Zealand. *Journal of Hydrology (New Zealand)*, Vol. 51(No. 2), 111-120. Retrieved from <https://www.jstor.org/stable/43945036>
- HRU. (1972). *Design Flood Determination in South Africa*. University of Witwatersrand, RSA, Department of Civil Engineering.
- Hydrology Studio. (n.d.). *The Rational Method*. Retrieved from <https://www.hydrologystudio.com/rational-method/#:~:text=According%20to%20documented%20history%2C%20the,on%20how%20to%20apply%20it.>
- Jones, H. S. (2018). *National Environmental Standards for Plantation Forestry commence*. Retrieved from Beehive.govt.nz: <https://www.beehive.govt.nz/release/national-environmental-standards-plantation-forestry-commence>
- Keller, G., & Sherar, J. (2003). *Low-volume roads engineering: Best management practices field guide*. Retrieved from <https://vtechworks.lib.vt.edu/handle/10919/68420>
- Ladson, T. (2017). *[BLOG] On the calculation of equal area slope*. Retrieved from <https://tonyladson.wordpress.com/2017/03/04/on-the-calculation-of-equal-area-slope/>
- Landcare Research. (2020). *Distribution of Pumice Soils*. Retrieved from SoilsMapView: https://soils-maps.landcareresearch.co.nz/?layername=fsl_nzsc&idcolumn=nzsc_order&idvalue=M&mapfile=fsl&srs=EPSG:2193&mode=normal
- Mata-Lima, H., Vargas, H., Carvalho, J., Gonçalves, M., Caetano, H., Marques, A., & Raminhos, C. (2007). Comportamento hidrológico de bacias hidrográficas: integração de métodos e aplicação a um estudo de caso. *Rem: Revista Escola de Minas*(60(3)), 525-536.

- McCormack, D. (2020). *The comparison of 3 flood flow estimation methods within New Zealand*.
- Ministry for Primary Industries. (2020). *National Environmental Standards for Plantation Forestry*. Retrieved from <https://www.mpi.govt.nz/forestry/national-environmental-standards-plantation-forestry/>
- Ministry for the Environment. (2004). *On-Site Stormwater Management Guideline*. Retrieved from https://www.waternz.org.nz/Attachment?Action=Download&Attachment_id=2967
- Ministry for the Environment. (2018). *About the National Environmental Standards for Plantation Forestry*. Retrieved from <https://www.mfe.govt.nz/land/land-acts-and-regulations/national-environmental-standards-plantation-forestry/about-standards>
- Ministry of Works and Development. (1978). *Culvert Manual Volume 1*. Civil Division Publication CDP 706/ A.
- Ministry of Works and Development. (1980). *A method for estimating design peak discharge (Technical Memorandum No. 61)*. Retrieved from https://docs.niwa.co.nz/library/public/TM61_1980.pdf
- NEESON, T., GORMAN, A., WHITING, P., & KOONCE, J. (2008). Factors Affecting Accuracy of Stream Channel Slope Estimates. *North American Journal of Fisheries Management*, 28(3), 722-732. doi:<https://doi.org/10.1577/M05-127.1>
- NIWA. (n.d.). Retrieved from High Intensity Rainfall Design System V4: <https://hirds.niwa.co.nz/>
- NIWA. (2019). *New Zealand River Flood Statistics*. Retrieved from <https://niwa.maps.arcgis.com/apps/webappviewer/index.html?id=933e8f24fe9140f99dfb57173087f27d>
- NOMOGRAM. (n.d.). Retrieved from Definitions.net: <https://www.definitions.net/definition/NOMOGRAM>
- Normann, J., Houghtalen, R., & Johnston, W. (1985). *Hydraulic Design of Highway Culverts*. United States. Federal Highway Administration. Retrieved from <https://rosap.nhtl.bts.gov/view/dot/54219>
- NZFOA. (2020). *NZ Forest Road Engineering Manual*. Retrieved from <https://docs.nzfoa.org.nz/live/nz-forest-road-engineering-manual/8-river-crossings/>
- Oregon.gov. (2014). *Appendix F - Rational Method*. Retrieved from <https://www.oregon.gov/ODOT/GeoEnvironmental/Pages/Hydraulics-Manual.aspx>
- Pendly, M., Bloomberg, M., & Visser, R. (2015). Investigating the regional variation in rules and best management practices for forestry in New Zealand. *Australasian Journal of Environmental Management*, 22(3), 298-314.
- Pennington, M. (2012). The Rational Method - Frequently Used, Often Misused. *Water New Zealand Stormwater Conference 2012* .

- Ravazzani, G., Boscarello, L., Cislighi, A., & Mancini, M. (2019). Review of Time-of-Concentration Equations and a New Proposal in Italy. *Journal of Hydrologic Engineering*(24(10)). doi:10.1061/(ASCE)HE.1943-5584.0001818.
- Sharifi, S., & Hosseini, S. (2011). Methodology for Identifying the Best Equations for Estimating the Time of Concentration of Watersheds in a Particular Region. *Journal of irrigation and drainage engineering*(137(11)), 712-719. doi:https://doi.org/10.1061/(ASCE)IR.1943-4774.0000373
- Smart, P. (2004). *HydroCAD*. Retrieved from Understanding Hydrology : <https://www.hydrocad.net/understanding.htm>
- Sturtevant, L. (2017). *using the Flow Length tool in Spatial Analyst's Hydrology Toolbox to find the Longest Flow Path*. Retrieved from ESRI: <https://community.esri.com/t5/arcgis-spatial-analyst-questions/using-the-flow-length-tool-in-spatial-analyst-s-hydrology/td-p/650360>
- The Engineering Toolbox*. (2008). Retrieved from Empirical Equations: https://www.engineeringtoolbox.com/empirical-equations-d_1400.html
- Thomason, C. (2019). *Hydraulic Design Manual*. Texas Department of Transportation. Retrieved from http://onlinemanuals.txdot.gov/txdomanuals/hyd/manual_notice.htm
- United States Bureau of Reclamation. (1987). *Design of small dams*. US Department of the Interior, Bureau of Reclamation. Retrieved from https://www.google.co.nz/books/edition/Design_of_Small_Dams/o4ZY-np1phIC?hl=en&gbpv=0
- US Army Corps of Engineers. (n.d.). *HEC-GeoHMS*. Retrieved from <https://www.hec.usace.army.mil/software/hec-geohms/>
- Vianello, A., Cavalli, M., & Tarolli, P. (2009). LiDAR-derived slopes for headwater channel network analysis. *Catena*, 76(2), 97-106. doi:https://doi.org/10.1016/j.catena.2008.09.012
- Waugh, J. (1972). *Report on the use of Technical Memorandum No. 61 (3rd Rev.) for estimating flood peak discharge for small and rural catchments in the Northland-Auckland area*. Water and soil Division, Ministry of Works and Development.

Appendices

Appendix A: Python Code

```
import arcpy
from arcpy.sa import *
from arcpy import env

# Path to watershed polygon
watershed = arcpy.GetParameterAsText(0)
# Path to DEM
dem = arcpy.GetParameterAsText(1)
# path to flow direction
fdrClip = arcpy.GetParameterAsText(2)
# path to output workspace
env.workspace =
"C:\\Users\\Luke\\Desktop\\410_arc_work\\Geo_database\\Banks_Catch.gdb"

# Empty container for intermediate data
intermediate = []

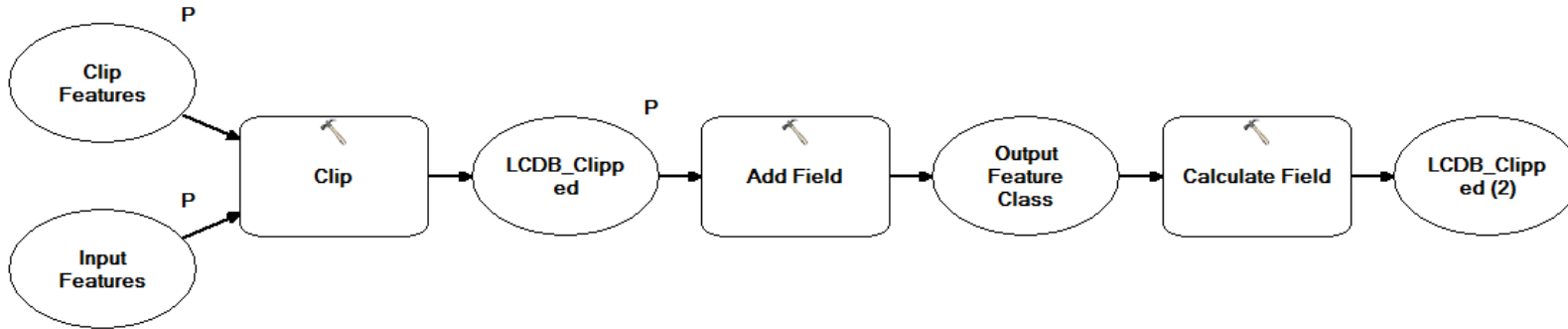
#message in arc
arcpy.SetProgressorLabel("Computing longest flow path for the basin...")

# Compute a downstream flow length raster
flowLength = Int(FlowLength(fdrClip, "DOWNSTREAM"))
arcpy.CalculateStatistics_management(flowLength)
# Get the maximum cell value from the flow length
maxValue = int(arcpy.GetRasterProperties_management(flowLength,
"MAXIMUM").getOutput(0))
# Return the maximum cell from flow length
maxCell = Con(flowLength, "1", where_clause="Value =
{}".format(repr(maxValue)))

# Use cost path to compute raster line from the max cell
lfpRas = CostPath(maxCell, dem, fdrClip, destination_field="Value")
intermediate.append(lfpRas)
# Generate a polyline from the cost path raster
rasLine = arcpy.RasterToPolyline_conversion(lfpRas, "rasLine", "ZERO",
simplify="NO_SIMPLIFY")
intermediate.append(rasLine)
# Dissolve the polyline to generate a single longest flow path line
lfp = arcpy.Dissolve_management(rasLine, "Longest_Flow_Path")
arcpy.AddSurfaceInformation_3d(lfp, dem,
"Z_MIN;Z_MAX;MIN_SLOPE;MAX_SLOPE;AVG_SLOPE", "BILINEAR", "", "1", "0")
intermediate.append(lfp)
```

Appendix B: Runoff Coefficient Processes

Part 1:



Part 2:

